Engineering Failure Analysis 62 (2016) 208–231

Contents lists available at ScienceDirect

Engineering Failure Analysis

journal homepage: www.elsevier.com/locate/engfailanal

Review

The fatigue of impellers and blades

Ming Zhang [a,b,c], Yan Liu [a,c], Weiqiang Wang [a,c,*], Pengfei Wang [a,c], Jianfeng Li [a,d]

[a] School of Mechanical Engineering, Shandong University, 17923 Jingshi Road, Jinan 250061, China
[b] School of Mechanical & Automotive Engineering, Qilu University of Technology, 3501 Daxue Road, Jinan 250353, China
[c] Engineering and Technology Research Center for Special Equipment Safety of Shandong Province, 17923 Jingshi Road, Jinan 250061, China
[d] Key Laboratory of High Efficiency and Clean Mechanical Manufacture of Ministry of Education, 17923 Jingshi Road, Jinan 250061, China

ARTICLE INFO

Article history:
Received 14 July 2015
Received in revised form 22 January 2016
Accepted 1 February 2016
Available online 6 February 2016

Keywords:
Impellers and blades
Fatigue failure
Fatigue load
Crack growth simulation
Fatigue test

ABSTRACT

Impellers and blades are the key components of turbomachines, and fatigue is the main failure mode of impellers and blades. The status and progress of fatigue research on impellers and blades were systematically introduced through reviewing fatigue failures, numerical simulations of fatigue, and fatigue tests of impellers and blades in several typical turbomachines. High cycle fatigue caused by vibration was the main failure mechanism, and fatigue cracks usually initiated from the location of stress concentration. The resonance caused by the aerodynamic load was the main cause of fatigue failure of impellers and blades in a steady operating condition. The coupling of the meshless method and the finite element method and the combined fatigue test of actual impellers and blades are the developmental direction and research focus of the future.

Contents

* Corresponding author at: School of Mechanical Engineering, Shandong University, 17923 Jingshi Road, Jinan 250061, China.
E-mail address: wqwang@sdu.edu.cn (W. Wang).

http://dx.doi.org/10.1016/j.engfailanal.2016.02.001

1. Introduction

Turbomachines play an important role in heavy industry, and have been widely used as the core driving force in aviation, energy, oil refining, petrochemical, coal chemical, natural gas transportation, metallurgy, and other important areas. The failures of impellers and blades (I&B) which are the key components of turbomachines not only cause significant economic losses to enterprises and society, but also threaten people's lives. In addition, there are many fundamental scientific problems about the failures of I&B. Therefore, research on failures, especially on fatigue, which is the main failure mode of I&B, provides references for the design, manufacture, application, inspection, monitoring, and remanufacturing of I&B. Moreover, the study of the fatigue of I&B is beneficial to guarantee the safe operation of turbomachines and gives supports to intense research on relevant fundamental scientific problems.

Failures of I&B mean that I&B cannot work properly, and include two situations: I&B are severely damaged and unable to work, or I&B cannot efficiently and reliably work. I&B with periodic structures have characteristics of complex geometries, various structural forms, poor working conditions, and multi-field coupling effects in operations. Also, there are many adverse factors in the design, manufacture, and service of I&B which induce I&B to fail. So failures of I&B present the characteristics of multiformity, complexity, and severity.

Failures of I&B are caused by the combined action of “internal reason” and “external reason”. The “external reason” mainly refers to the environmental factor, which includes load, temperature, and medium. The “external reason” is different in various applications. For example, temperature has an important effect on the failures of I&B serving at high temperature [1–3]. Steam turbine blades in the low pressure area work under more adverse conditions and the failure seems to occur more easily than blades in the high or medium pressure areas [4]. The “internal reason” heavily affects failures, and it usually refers to the situation of I&B themselves, which includes material, structure, and processing technology [5–7]. For example, the connection method of disk and blade has a great effect on failures of I&B [8–16].

The difference of “external reason”, such as the alternating load, corrosive medium, erosion medium, and high temperature, leads to the different failure mechanisms of I&B, which usually involve fatigue, corrosion, creep, wear, foreign object damage (FOD), and the combined action of these mechanisms [17–24]. The failure mechanisms are very different for different “external reasons” in various service environments [25–28]. The “internal reason” mainly affects the failure mode, especially the failure position. Fracture, cracking, thinning, and deformation are the main failure modes of I&B, as shown in Fig. 1. Cracking and fracture are more common, and can be caused by most of the above failure mechanisms. Thinning and deformation are relatively rare. Thinning usually appears in situations of serious wear or corrosion, for example, solid particles carried in the air increase blade thinning of centrifugal compressor impellers. Deformation can appear in the fabrication process, such as welding, but it appears

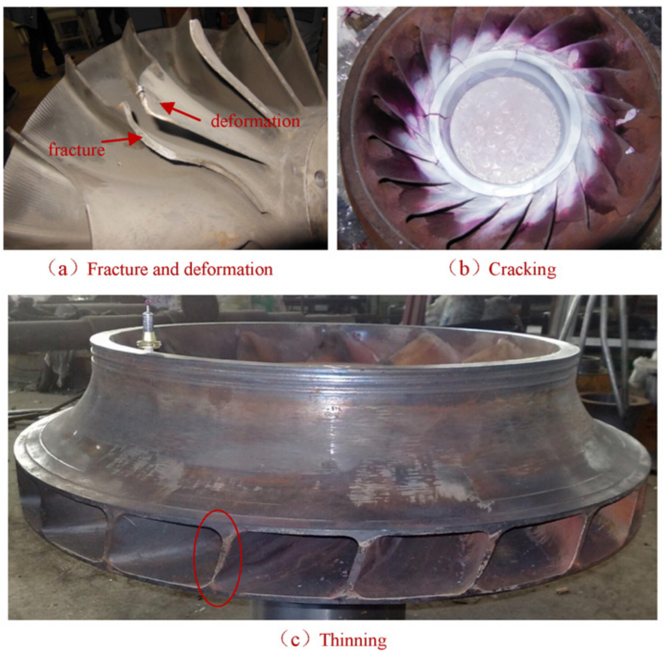

Fig. 1. The main failure modes of I&B.

more commonly in service due to the superposition of various loads. In addition, deformations such as dents or bulges also occur after FOD.

Fatigue is the most important failure mechanism of I&B [29]. In this paper, we will present a review of fatigue failures, numerical simulations of fatigue, and fatigue tests of I&B in typical turbomachines, and systematically introduce the status and the development of fatigue research on I&B.

2. Fatigue failures of the typical I&B

We want to present an insightful overview on the fatigue failures of I&B including failure mechanisms, failure modes, dangerous positions, and failure reasons. We chose the I&B of a centrifugal compressor, axial compressor, steam turbine, flue gas turbine, aero-engine compressor, aero-engine turbine, and gas turbine as the investigation objects.

2.1. Fatigue failures of centrifugal compressor impellers

In 1986, Hu et al. [30] analyzed the fatigue fracture of the first stage SNCM 5 impeller of a high pressure cylinder of the 103-JHP (the position number of the compressor in the unit) turbine compressor in a fertilizer plant. The compressor had been running for two years and suffered 32 cycles of shutdown and startup until the accident happened in 1982. Hu concluded that the reason of failure was fatigue induced by stress concentration. In addition, he indicated that the change of working conditions resulted in axial stress, increased uneven wear of shroud and uneven riveting, and caused stress concentration.

A fatigue crack usually initiates from the position of stress concentration. For a centrifugal compressor impeller, a fatigue crack generally initiates from the blade root because stress concentration and large load usually appear in this area. In 2007, Cheng [31] reported an accident in which all of the inlet blades of an Ingersoll-Rand nitric oxide centrifugal compressor AISI410 impeller fractured along the roots. In 2010, S. Sivaprasad [32] found that the fatigue crack appeared at the blade root in the fracture accident of a first stage impeller in a X4CrNi13-4 air compressor, as shown in Fig. 2.

Stress concentration accelerates the initiation of fatigue crack, which is usually caused by riveting, welding, composition segregation, porous material, abnormal microstructure, and pits. In Hu's [30] analysis, fatigue cracks mostly initiated from the thin walls of rivet holes at the blade tip, and the uneven riveting of blade and shroud resulted in stress concentration and induced the initiation of fatigue cracks. In 2000, Dong et al. [15] analyzed the failures of the third to the fifth stage of a Cr13Ni6MoNb copper-based brazing impeller in three air turbine compressors, and found that the fatigue cracks initiated from defects formed by the brazing and the composition segregation area in the brazing seam. In 2005, Hou et al. [33] analyzed one of the first stage and second stage 34CrNi3Mo impellers in eight H240-9.5/0.98 centrifugal compressors, in which fatigue failures happened many times, and found that cracks initiated from welding craters in the welding heat affected zone between the shroud and blade. In 2006, Wang et al. [34] investigated fatigue cracking of a second stage impeller in a centrifugal compressor, and they found surface decarbonization, abnormal microstructure, and a lot of ferrites in the fracture origin zone. In 2009, Wang et al. [35] analyzed a blade fracture of a first stage impeller in a centrifugal compressor, and concluded that the fatigue crack initiated from a pit on the blade pressure surface which was caused by FOD. In 2011, Chen et al. [36] analyzed a blade fracture of a first stage impeller in an air compressor, and indicated that the fatigue crack initiated from a corrosion pit.

Vibration is the main reason for fatigue failures in centrifugal compressor impellers. In 2003, Xiong [37] concluded that vibration fatigue resulted in several failures of H240-9.5/0.98 centrifugal compressor impellers. In 2004, Qi [38] analyzed vibration fatigue of DHP56-1 centrifugal compressor blades which work in the resonance region. In the former report of Cheng [31], he indicated that vibration fatigue of the blade was caused by the intensified dynamic imbalance of the impeller due to a fracture of the fastening bolt with improper material. In 2009, Hu [39] concluded that vibration resulted in fatigue failure of a centrifugal compressor impeller. In 2010, S. Sivaprasad [32] supposed that fatigue failure of an air compressor impeller was caused by the intensified vibration which resulted from unstable transient operation. In 2011, Ma et al. [40] analyzed the high cycle fatigue of a second stage impeller blade of a HLR806-2 centrifugal compressor in an air separation unit, and found that the vibration load

(a) Profile at the impeller (b) Profile at the blade root

Fig. 2. Fatigue cracking of centrifugal compressor impeller at the blade root [32].

was caused by the scale layer on the local blade surface because the blades were impacted by particles from aluminum fins on the interstage cooler tubes.

The corrosive medium has important effects on fatigue failures of centrifugal compressor impellers. In the preceding report of Cheng [31], he found that the fastening bolt underwent corrosion cracking. Hu's above analysis [39] indicated that corrosion fatigue cracking occurs under the action of hydrogen sulfide in the centrifugal compressor impeller.

2.2. Fatigue failures of axial compressor impellers

Fatigue failures of axial compressor impellers are similar to centrifugal compressor impellers', and vibration is also the main reason of fatigue failures. In addition, the blade root seems to be in a dangerous position where the fatigue crack easily initiates, and corrosion accelerates fatigue failure. In 2006, Dai et al. [41] analyzed first stage blade fractures at the bottom of the blade profile 10 mm from the root where fractures happened many times. Finite element calculation showed that the blade resonance caused by the low frequency excitation force was likely to occur, and the bending stress caused by the air flow was close to the allowable stress limit. In 2007, Xie [42] analyzed three fracture accidents of first stage rotor blades of a AG060/14L5 axial–centrifugal multiplex compressor in a catalytic cracking unit, and found that all the fatigue fractures appeared at the blade root and the cracks initiated from corrosion pits. In 2009, Fu [43] investigated blade fracture of a Z1600-0.245/0.0961 axial compressor, and concluded that the accident was caused by the blade resonance. In 2011, Zhi et al. [44] reported fatigue fracture accidents of two rotor blades of a ninth stage impeller in an axial air compressor. The fractures occurred in the position of the transition arc at the blade root.

2.3. Fatigue failures of steam turbine blades

In 1985, Zhang et al. [45] analyzed some blade fatigue accidents of a synthesis gas compressor turbine in a fertilizer plant. Vibration was the main reason of steam turbine blade fatigue which was similar to the situations of the centrifugal compressor impeller and axial compressor impeller. In 2005, Weng [46] analyzed a tenth stage blade fracture of a FCC25-3.43/2.0/0.9 steam turbine. The fracture morphology is shown in Fig. 3. He concluded that high cycle fatigue was due to the abnormal vibration of the blade caused by the extracted steam and the frequent change of load. In 2007, E. Poursaeidi et al. [47] found that the blade failure of a generator rotor turbine was caused by the blade resonance because of the unsteady aerodynamic force. In 2011, H. Kim [48] analyzed fatigue failure of a fourth stage blade in a low pressure steam turbine caused by vibration.

High temperature steam is the major medium of a steam turbine, and poor quality of steam may results in the corrosion of blades. Corrosion fatigue seems to be a typical failure mode of steam turbine blades. In 1990, Zhao [49] analyzed the blade fracture of a steam turbine which was a part of a KT1202 air compressor in a fertilizer plant and found that there were some corrosion pits on the blade pressure surface, and a lot of Si, P, S, and other acidic substances were detected on the fatigue fracture. In 1997, Li et al. [50] analyzed corrosion fatigue of a fourteenth stage blade of a steam turbine, and found that there were a lot of corrosion pits and corrosion products on the fractured blade. The higher Si content in the precipitates on the blade surface indicated that there were a lot of impurities in the water, and the very low Cr content in the corrosion pit of the fracture origin zone indicated the poor corrosion resistance of the blade material. In 1998, Zhou [51] investigated a fracture of a second to last stage blade in a N200-130/535/535 steam turbine, and found that the characteristics of corrosion fatigue appeared on the fracture. In addition, corrosion pits and corrosion traces caused by Cl were observed. In 2003, G. Das et al. [52] analyzed the failure of a low pressure turbine blade in a thermal power plant. The blade material was tempered martensitic stainless steel. A Si rich phase was found on the blade surface, there were some pits and grooves on the blade edge, and Cl was detected in the pits, so they thought the intergranular fracture resulted from corrosion fatigue. In 2005, You et al. [53] analyzed a last stage blade fracture of a steam turbine. They found that the crack initiated from the leading edge near the blade pressure surface, but not from corrosion pits. Intergranular fracture morphology appeared outside the fatigue area, and there were some corrosion products with a lot of S and Cl on the intergranular surface. The crack had obvious bifurcations, and there were a lot of corrosion pits on the

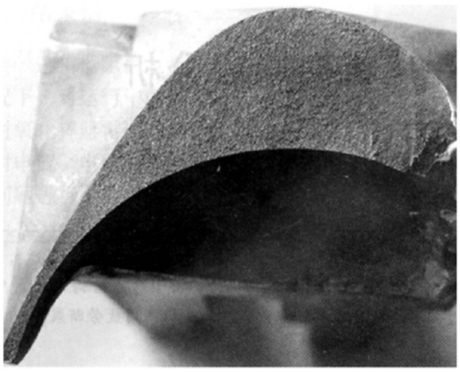

Fig. 3. Fracture morphology of the blade [46].

blade suction surface. So the failure mechanism seemed to be stress corrosion cracking. In 2007, Chen et al. [54] studied the cracks in 85 blades of a last stage, which were in the low pressure area of a N135-13.24/535/535 135 MW steam turbine. The cracks were mainly caused by corrosion fatigue or stress corrosion, the long cracks usually seemed to be fatigue cracks. The features of corrosion fatigue appeared on the fractures, and the features of stress corrosion were obvious for the short cracks or at the beginning stage of cracks. In 2007, Wang et al. [55] analyzed the fatigue of a last stage blade in a steam turbine, and concluded that corrosion accelerated the growth of the fatigue crack. In H. Kim's [48] analysis above, cracks initiated from corrosion pits on the leading edge of the blade, as shown in Fig. 4. A lot of Cl and Na were detected in the pits, and the reason for corrosion seemed to be a small leak of seawater in the condenser tube.

Generally, there are some small droplets in the medium, so stress concentration and further fatigue failures are probably caused by water erosion. In 2011, Liu et al. [56] investigated a fracture of a turbine blade in a thermal power plant, and found that a crack initiated from a water erosion pit on the trailing edge of the blade.

For steam turbines, the service environment is usually more dangerous in the low pressure area than in the high or medium pressure area. So, fatigue failures in low pressure areas are more common, especially for failures of the second to last or the last stage blade in low pressure areas. In 2011, Yang et al. [57] analyzed a fatigue fracture of a last stage blade in a steam turbine. In the above analyses of H. Kim, Zhou, G. Das, You, Liu, Wang, et al., fatigue failures also appeared in the second to last or the last stage blade in low pressure areas.

Z. Mazur et al. [10,58,59] analyzed several fatigue failures of steam turbine blades, and concluded that blade vibration caused by unsteady fluid was the main failure reason when a steam turbine operates below the design condition. In addition, all of the fractures analyzed by Z. Mazur occurred in the last stage of a steam turbine, and the cracks initiated from the root of the trailing edge. The last stage blade morphology of a steam turbine and the blade fracture position are shown in Fig. 5. In addition, erosion and corrosion caused by circular steam accelerate the propagation of fatigue cracks. The above points are the main failure features of steam turbine blades.

Low cycle fatigue failures of steam turbine blades are relatively less. In 2009, J. Kubiak [60] analyzed a low cycle fatigue failure of a steam turbine blade, and found that the crack initiated from the secure pinhole of the blade root due to large thermal stress. The cracked blade is shown in Fig. 6.

2.4. Fatigue failures of flue gas turbine blades

The medium composition of flue gas turbines is complex, compared with that of centrifugal compressors and axial compressors, so corrosion or erosion has significant effects on fatigue failure of flue gas turbine blades. In 2005, Chen [61] investigated the corrosion fatigue failure of a rotor blade in a YLII-7000A double-stage flue gas turbine. The combined action of the S corrosion at high temperature and the high local stress resulted in crack initiation. In 2006, Hao et al. [62] concluded that corrosion under high temperature combustion conditions led to the failure of the tenon and the final fracture of rotor blades in a flue gas turbine.

The connection method of tenon/mortise is widely used in flue gas turbines, and fatigue cracks easily initiate from the tenon or the mortise because of stress concentration. In 2005, Gai et al. [63] analyzed a fracture of YLII-10000K flue gas turbine blades, and found that fatigue cracks initiated from the tenon edge and the tenon root. In 2005, Chen et al. [64] analyzed the failure of a first stage rotor blade in TP3142/2.36-1.146, a top gas pressure recovery turbine, and found that there were some cracks on the blade tenon due to bad contact and other reasons. According to the analysis of Hao [62] mentioned above, local serious wear due to the uneven contact between tenon and mortise leads to initiation of fatigue cracks, and the mixed grain and the continuous coarse carbide film on the grain boundary in each part of the tenon accelerate the initiation and the propagation of cracks. In 2007, Han et al. [65] investigated blade failure of a flue gas turbine, and concluded that the small contact area and the non-uniform contact between tenon and mortise, and the damage of the grain boundary accelerated the growth of cracks. Hu et al. [66,67] analyzed fretting fatigue of a flue gas turbine rotor blade, and concluded that fretting caused by large local stress due to the bad assembly between tenon and mortise was the major reason of fatigue fracture.

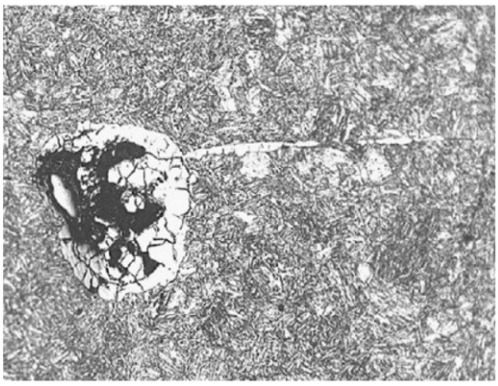

Fig. 4. Microstructure of corrosion pit [48].

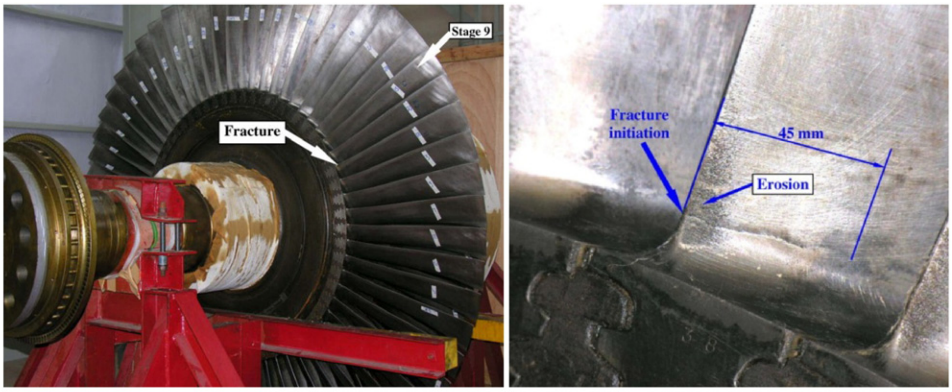

(a) Morphology of last stage blades (b) Fracture position of the 38# blade

Fig. 5. Morphology of last stage blades and fracture position of the blade [59].

2.5. Fatigue failures of aero-engine compressor blades

Vibration is also the primary cause of fatigue damage of aero-engine compressor blades, just like the situations of some I&B mentioned above. In 2006, Li et al. [68] surveyed a failure of a fourth stage rotor blade in an aero-engine compressor, and found that blade fatigue was caused by vibration stress. In 2006, Wu et al. [69] analyzed a first stage rotor blade fracture of a compressor, and indicated that the improper angle of the zero order adjustable blade resulted in vibration fatigue of the blade. In 2007, Liu [70] investigated low cycle fatigue of first stage compressor rotor blades in an aero-engine, and considered that flutter was the major failure reason. In 2008, Zang et al. [71] analyzed the cracking of the leading edge of a blade at the front row rectifier in a compressor, and concluded that abnormal vibration led to the failure. Lv et al. [72] reported a vibration fatigue failure of aero-engine compressor blades. The failed blades are shown in Fig. 7. In 2011, Jiang et al. [73] studied high cycle vibration fatigue of third stage rotor blades in an aero-engine compressor.

Fatigue cracks usually initiate from a position of stress concentration, and the reasons of stress concentration include material microstructural defects, mechanical abrasion, and FOD. In 2006, Wu et al. [69] analyzed the fracture of a first stage rotor blade in a compressor, and found that the fatigue crack initiated from the position of mechanical abrasion on the blade suction surface. In 2007, N. Ejaz et al. [74] analyzed a blade fall-off accident of a single stage compressor in an aero-engine, and found that the fatigue crack initiated from a forging defect at the blade root. In 2009, V. Infante et al. [75] surveyed a blade fracture of a fifth stage high pressure compressor. The blade material was nickel base superalloy, and cracks initiated from a material defect on the leading edge. The stress concentration of aero-engine compressor blades is mainly caused by corrosion or FOD. In 2009, L. Witek et al. [76] studied the failure of a helicopter engine blade, and discovered that the fatigue crack initiated from a corrosion pit on the leading edge. The fractured blade is shown in Fig. 8. In the former analyses of Li, Jiang, Lv, Liu, et al., all the cracks initiated from corrosion pits. But, in the analyses of E. Silveira, V. Infante, et al., cracks initiate from pits caused by FOD.

The assembly of tenon and mortise is the primary connection method of aero-engine compressors, and fatigue cracks easily initiate from this location. In 2005, Yu et al. [77] reported a fracture accident of a first stage blade in an aero-engine compressor, and there were some obvious longitudinal fretting marks on the tenon/mortise. The serious swing of a blade with improper clearance between tenon and mortise is the main reason of fatigue failure. The bad assembly of tenon and mortise usually results in fretting fatigue failure [11,78–82], which is the common failure mode in aero-engine compressors.

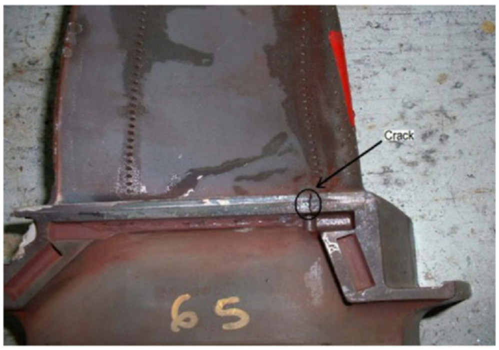

Fig. 6. Crack of a first stage rotor blade [60].

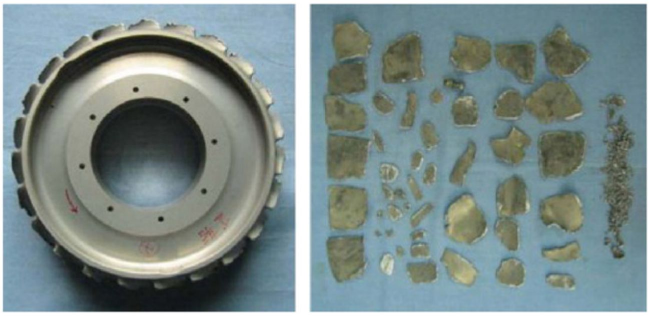

Fig. 7. Debris of the first stage rotor and the first stage rotor blades [72].

Low cycle fatigue is an important failure mode of aero-engine compressor blade because of the frequent taking off and landing of aircraft or the bad assembly of tenon and mortise. In 2007, K. S. Song et al. [83] surveyed fatigue fractures of rotor blades in a J79 engine compressor, as shown in Fig. 9, and there were several fatigue origins and secondary cracks on the fracture, as shown in Fig. 10. The reason for fracture seemed to be low cycle fatigue caused by a serious rotating stall. In Yu's analysis [77], failure was also low cycle fatigue caused by the bad assembly of tenon and mortise.

2.6. Fatigue failures of aero-engine turbine blades

Vibration is also a main reason of fatigue failure in aero-engine turbine blades. In 2005, Zhong et al. [84] found that the large clearance of adjacent blades resulted in blade fractures due to bending vibration fatigue. In 2005, Liu et al. [85] surveyed some vibration fatigue fractures of third stage turbine blades in an aero-engine. In 2006, S. K. Bhaumik et al. [86] studied a failure of a low pressure turbine blade in an aero-engine. The failed blade is shown in Fig. 11. They found that the fatigue crack initiated from the transition arc of the blade coating, and was caused by vibration. In 2007, Wang et al. [87] analyzed a tenon fracture of a third stage turbine blade in an aero-engine, and concluded that the failure was related to large bending stress caused by blade vibration due to large clearance of a few neighboring shrouds.

The ambient service temperature of aero-engine turbines is up to several hundreds or even a thousand degrees centigrade, and high temperature has important effects on fatigue failures. Creep fatigue is a typical failure mode of aero-engine turbine blades. The low yield strength and the insufficient strength of the grain boundary are the major causes of creep fatigue. In 2002, I. Salam et al. [26] surveyed a fracture of a second stage turbine blade in a fighter. They discovered that a W-shape crack initiated from the blade surface because the creep resulted in the grain boundary sliding, as shown in Fig. 12, and concluded that the subsequent low cycle fatigue fracture was caused by a rotating stall or a surge. In 2002, M. Park et al. [88] investigated a failure of a J69-T-25 turbojet engine turbine blade, as shown in Fig. 13. They found that a crack initiated from a position of surface friction, and the blade was damaged and discolored due to the action of thermal air flow. The thermal effect resulted in the coarse γ-phase in the nickel base superalloy and a decrease of fatigue strength of the matrix material. In the former analyses of Zhong [84] and Wang [87], creep had significant effects on fatigue. E. Silveira et al. [89,90] analyzed thermal mechanical fatigue failure of an aero-engine high pressure turbine, and found that a crack initiated from a cooling hole. The blade fracture is shown in Fig. 14. The blade material was a precipitated hardened nickel base alloy, and they thought that the large carbides of hafnium and tantalum accelerated the fracture of the blade. In 2006, N. Ejaz et al. [91] surveyed local fall-block failures of two blades in a turbine engine, as shown in Fig. 15. The blade was made of Udimet 500 without a superficial coating. They considered that the intergranular crack of the blade was formed due to high temperature, and found that the crack on the blade suction surface was close to the high

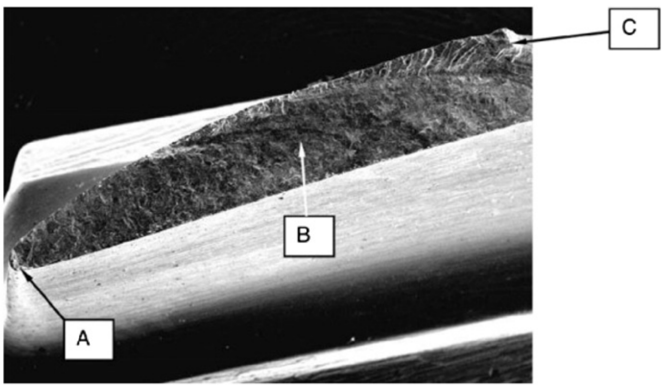

Fig. 8. View of a fractured blade with marked crack origin zone (A), fatigue fracture area (B) and rupture zone (C) [76].

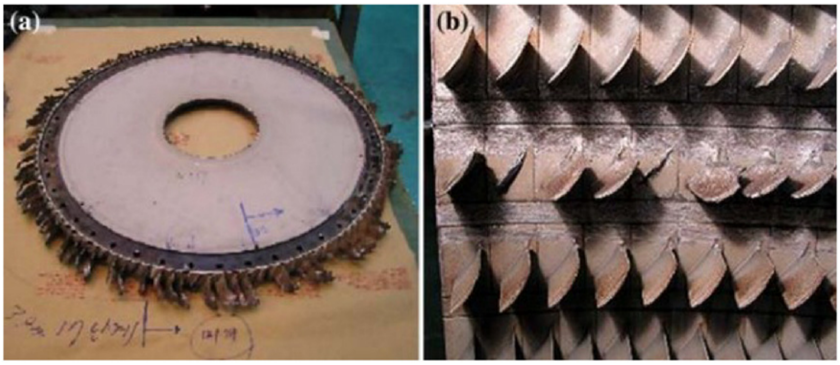

(a) 17^{th} stage rotor blades (b) Stationary blades

Fig. 9. J79 engine compressor rotor blades [83].

stress area. In addition, they concluded that the crack initiated from the grain boundary due to oxidation corrosion, the high temperature led to microstructure deterioration of the blade material, and the failure mechanism was high cycle fatigue after hot corrosion.

The material and processing technology of aero-engine turbines are different from the usual I&B′, so the fatigue of aero-engine turbine blades has special characteristics. Zhang et al. [92–94] investigated more than ten similar cracking or fracture accidents of second stage turbine blades. The results showed that cracks initiated from stress concentration positions caused by surface recrystallization or different microstructures in various parts of the blade. The complex profile of the blade caused distortion of the temperature field in the molding process which led to different microstructures. In 2011, He et al. [95] surveyed fractures of two blades in an aero-engine, as shown in Fig. 16, and considered that the cause of failure was recrystallization, which was caused by plastic deformation during the sandblasting process in solution annealing. In 2007, K. S. Song et al. [96] inspected a fracture of an aero-engine blade, as shown in Fig. 17, and concluded that unreasonable processing technology caused the separation of Ti and Mo, induced stress concentration, and finally resulted in fatigue failure. In 2008, Hou et al. [97] studied the effects of crystal orientation on the fatigue life of single crystal turbine blades. In 2009, H. Kim [98] analyzed fatigue fracture of the last stage blade in an aero-engine, as shown in Fig. 18. The blade was made of the directionally solidified nickel base superalloy MAR200Hf, and the crack initiated from the position of stress concentration caused by pores on the trailing edge and the segregation zone of hafnium and titanium.

The fatigue failure position of aero-engine turbines is similar to that of aero-engine compressors, and the positions of mechanical damage, corrosion pits, and junction of blade and disk easily cause fatigue cracking. In 2002, M. Park et al. [88] analyzed a failure of a J69-T-25 turbojet engine turbine blade, and found that the crack initiated from a position of surface friction. In 2008, N. J. Lourenco et al. [99] investigated an accident of a helicopter engine turbine, and found that a fatigue crack initiated from a corrosion pit on a fourth stage blade. In 2010, He et al. [100] surveyed fracture failure at the root of a titanium alloy rotor blade in an aero-engine, and considered that a high cycle fatigue crack was due to local stress of the blade, and the fretting accelerated the initiation of the fatigue crack. In 2010, I. Le May [101] analyzed a failure of a second stage blade of a helicopter, and found that a fatigue crack initiated from the junction of blade and disk. In 2011, Liu et al. [102] studied fatigue failure of a single crystal blade in an aero-engine, and concluded that the friction between blade tip and engine casing led to an alternating load in the position of stress concentration, and caused fatigue failure. In 2013, Qu et al. [103] analyzed a failure of a first stage

(a) Characteristics of multi-source fatigue (b) Secondary cracks

Fig. 10. Low cycle fatigue characteristics of a blade [83].

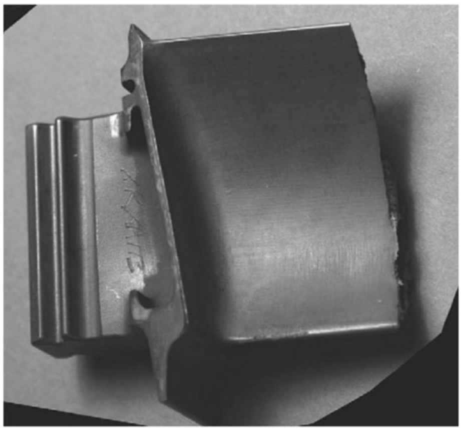

Fig. 11. Fracture of a low pressure turbine rotor blade [86].

rotor blade in an aero-engine turbine, and considered that a fatigue crack initiated from a position of stress concentration caused by a material defect on the trailing edge.

2.7. Fatigue failures of gas turbine blades

Gas turbine blades usually work at high temperature, and the high temperature has important effects on fatigue failures of gas turbine blades. In 2003, Yuan et al. [104] analyzed a fracture of a first stage turbine rotor blade in a gas turbine, and considered that thermal mechanical fatigue was the cause of blade fracture. In 2003, Jiang et al. [105] surveyed a fracture of a second stage turbine blade in a gas turbine, and concluded that the failure mode was low cycle fatigue which was related to the thermal stress caused by the extreme temperature of the fatigue origin zone in a short time period.

Vibration is also the primary cause of fatigue of gas turbine blades. In 2010, Y. S. Choi [106] analyzed the failure of a gas turbine during the startup phase, and fractures of the first four stage blades are shown in Fig. 19. The fatigue fracture of a first stage turbine blade occurred at the blade root due to resonance. In 2012, Song [107] studied failures of two blades breaking off in a low pressure compressor of a gas turbine and some tenons cracking in the same stage. The failures were caused by vibration fatigue. The fretting of the bad assembly of disk and blade was the main cause of blade vibration fatigue.

Particle erosion has important effects on the fatigue of gas turbine blades, as there are a lot of solid particles in the medium of a gas turbine. In 2006, Cui et al. [108] analyzed fractures of martensitic stainless ASTM403 blades in a gas turbine compressor, and considered that the pits were caused by particle erosion, and induced low cycle fatigue under the action of alternating stress.

2.8. Summary of I&B fatigue failures

Some resumes of fatigue failures including name of elements, failure mechanism, crack initiation zone, and main cause of failures are shown in Table 1.

Through reviewing numerous fatigue failures in centrifugal compressor, axial compressor, steam turbine, flue gas turbine, aero-engine compressor, aero-engine turbine, and gas turbine, we found that the fatigue failure mechanisms of I&B usually include high cycle fatigue, low cycle fatigue, corrosion fatigue, fretting fatigue, creep fatigue, and thermal mechanical fatigue.

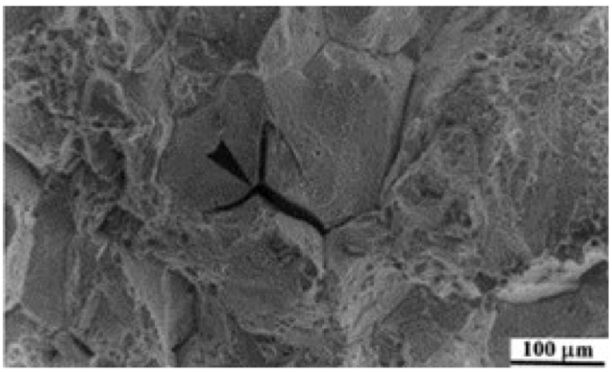

Fig. 12. Secondary crack with three points [26].

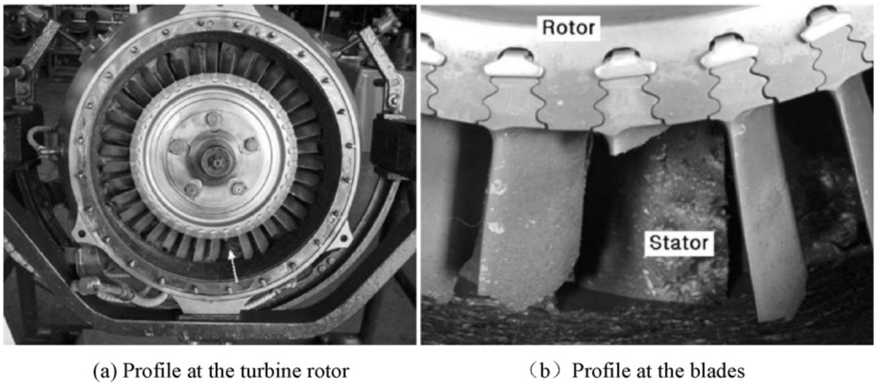

Fig. 13. Rear view of a J69-T-25 turbojet engine turbine [88].

Among them, high cycle fatigue caused by vibration is the main failure mechanism. For each type of I&B, the failure mechanisms are different due to the various service environments. Corrosion and high temperature in a service environment have significant effects on fatigue failures. For steam turbines, corrosion fatigue is an important failure mechanism due to the presences of S, Cl, and other corrosive mediums in the steam. For aero-engine turbines, creep fatigue is an important failure mechanism due to high temperatures in the service environment.

Fatigue failures only caused by an alternating load seem rare in numerous failures because of the rigorous anti-fatigue design of I&B. In fact, most fatigue failures are induced by stress concentration, which may be caused by structure, material defect, processing technology, corrosion, wear, and FOD. Therefore, improvements of material fatigue resistance and surface quality of I&B (such as hardness and corrosion resistance) are beneficial for the prevention of fatigue failures. As for failure position, fatigue cracks usually initiate from the blade root. For centrifugal compressor shrouded impellers, fatigue cracks usually initiate from the junction of blade and disk, or the junction of blade and shroud.

Fatigue life is different for different alternating loads. Low cycle fatigue of I&B is mainly caused by surge or a large change of centrifugal load during startup and shutdown. Low cycle fatigue occurs more often in aero-engine compressors or turbines due to the aircraft's frequent taking off and landing, and the large heat load. The high frequency vibration of blades caused by the weak agitation of air or the system vibration usually results in high cycle fatigue, which is the main failure mode of I&B. With the development of the economy and the enhancement of constraint of resources and environment, there is a higher requirement for the service life of I&B. Then the requirement of fatigue life of I&B should be more than 10^7 cycles and into the very high cycle regime in the future. However, current research on very high cycle fatigue of I&B is extremely limited. Therefore, we should intensify very high cycle fatigue research on I&B which has important significance to ensure a long operation life of I&B.

Based on the characteristics of fatigue failures of I&B, fatigue failures can be prevented from aspects of design, material, manufacture, assembly, operation, and overhaul.

(1) Design optimization is the basic method to avoid fatigue failures of I&B. The stress concentration is reduced and the stress remains at a safe level through the design optimization. The vibration modes of I&B should be fully considered to avoid possible resonance.
(2) Material is a key problem for the safe operation of I&B. The establishment of a fatigue property database of relevant I&B materials is necessary for the fatigue design of I&B. In addition, heat treatments must be carefully checked and the chemical composition, microstructures, mechanical properties, and defects of materials should meet relevant requirements.

Fig. 14. Upper view of the fracture surface of the blade that was identified as the origin of the failure [90].

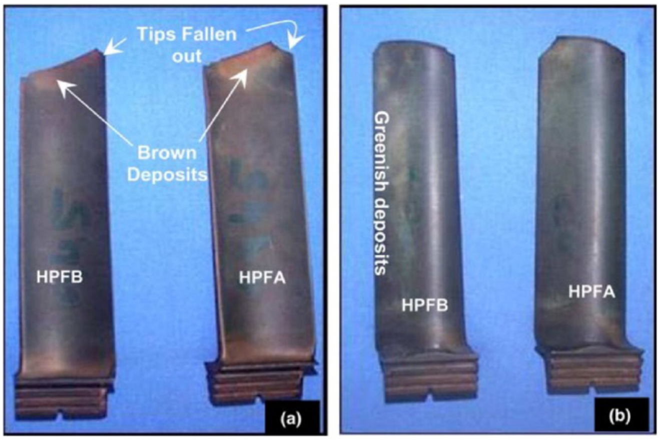

（a）Pressure surface （b）Suction surface

Fig. 15. Failed blades [91].

(3) Processing technologies have significant effects on the fatigue life of I&B. Processing technologies should be optimized and strictly inspected to ensure that the sizes, profiles, and surface roughness of I&B meet relevant requirements. Relevant anti-fatigue technologies such as shot blasting can be adopted to enhance the fatigue strength of I&B. Defects caused by processing should meet relevant standards, and the residual tensile stress should be relieved. Compared with heat treatments, the compensation of stress and strain can totally relieve the residual tensile stress and even induce the residual compressive stress.
(4) Assembly has significant effects on the fatigue life of I&B. A tight assembling increases the additional stress, and a loose assembling and blade mounting dislocation may cause abnormal vibration. Application of advanced assembling technology and strict inspection of assembling quality are necessary. Tests to measure frequency and dynamic balance after assembling are needed to reduce abnormal vibration.
(5) Operation conditions are also important for the safe operation of I&B. The improvement of operating conditions, such as the elimination of overload, low load, flutter, resonance, and water hammer and friction, is significant to reduce fatigue failures of I&B. For example, a decrease of oxygen in steam and the avoidance of high steam temperatures are effective in preventing high temperature fatigue of turbine blades in a high pressure area. The improvement of steam quality is the main method of eliminating corrosion fatigue of turbine blades in a low pressure area. In addition, the start, stop, loading and unloading of turbomachinery must gradually proceed, and the above processes should be carefully monitored and recorded. The unit should run near the optimal design condition. Operations deviating from the optimal design condition, particularly in the case of low load operation, usually increase the blade dynamic stress and unit vibration.
(6) A reasonable maintenance cycle of I&B and the detailed examination of each stage blades during overhaul are necessary. If some micro-cracks, obvious signs of corrosion, or high temperature oxidation are found, the blade should be repaired. We can adopt the methods of blade profile modification, operating condition adjustment, and even blade replacement to repair a cracked blade.

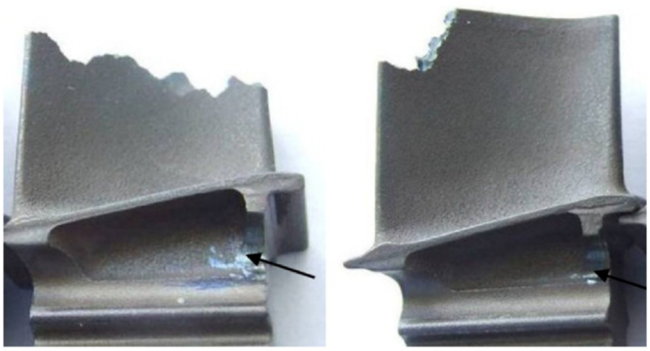

(a) No.14 blade (b) No.21 blade.

Fig. 16. Fractured blades [95].

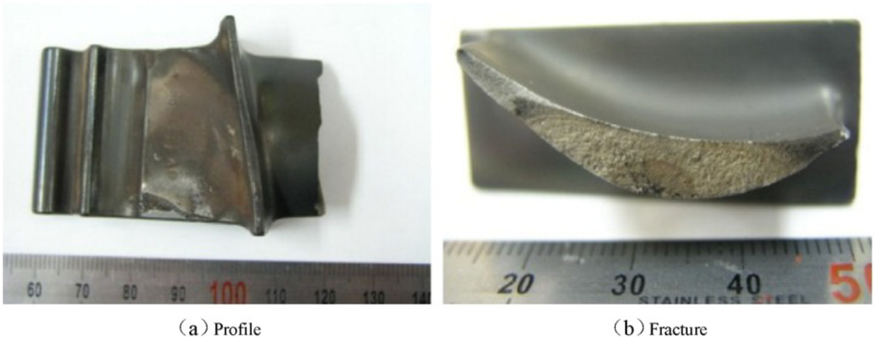

Fig. 17. Fractured blade [96].

3. Numerical simulations of the I&B fatigue

The load acting on the I&B is the most important "external reason" for fatigue failure, and the study of fatigue load has always been the focus of research. Fatigue loads of I&B usually include centrifugal load, aerodynamic load, temperature load, and vibration load. Fatigue loads can be obtained by theoretical calculations and tests, but it is difficult to measure vibration stress and strain of the assessment position of I&B in operation. In trial runs, the stress and strain can be measured, but there are some disadvantages such as the heavy workload, the complexity of the test system, and the difficulty of ensuring the accuracy of the data. So numerical analysis is the main method to determine assessment position and stress distribution of I&B.

In early stages, stress analyses of I&B were simple due to the limitation of relevant theories and computational methods [109–112]. With the development of computer technology, finite element analysis has been widely used in the mechanical analysis of I&B. Mechanical analysis of I&B usually includes static analysis for low cycle fatigue load, vibration analysis, and vibration response analysis.

Numerical simulations of fatigue crack growth significantly reduce the fatigue design time and the experimental costs, which is important in engineering. The most common numerical simulation methods of fatigue crack growth are the finite element method (FEM), the boundary element method (BEM), and the extended finite element method (XFEM).

3.1. The alternating load calculations of I&B

Mechanical analysis of I&B must involve centrifugal load. Centrifugal load analysis by the finite element method, which is highly accurate, provides theoretical references for the fatigue test, especially the low cycle fatigue test. In 1994, S. Aksoy et al. [113] analyzed the surface stress of an impeller under a centrifugal load by the finite element method, and confirmed the accuracy of test results. In 2006, Huang et al. [114] obtained the stress–speed curve of an impeller which provided theoretical references for the low cycle fatigue test. In 2009, Liu [115] studied the strength of a centrifugal compressor impeller under a centrifugal load, and analyzed the effects of the leading edge forms and the rounded angles of the contact edge of the blade and disk on the maximum stress of the blade.

The vibration caused by the aerodynamic load is an important part of the mechanical analysis of I&B, and a lot of failure analyses showed that most blade failures are caused by the superposition of vibration stress and centrifugal stress [116]. In 1971, J. Kirkhope et al. [117] proposed the finite element method for vibration analysis of the blade and disk. The waveform element with two nodes and a beam element replaced the disk and blade, respectively. But, application of this method is limited to the analysis of the low order vibration mode. In 2002, Hou et al. [118] conducted a mechanical analysis for the fatigue problem of a military engine turbine blade. They analyzed and evaluated the static stress and dynamic stress by the nonlinear finite element method after applying the centrifugal load, the aerodynamic load, the thermal expansion, and the contact of tenon and mortise. In

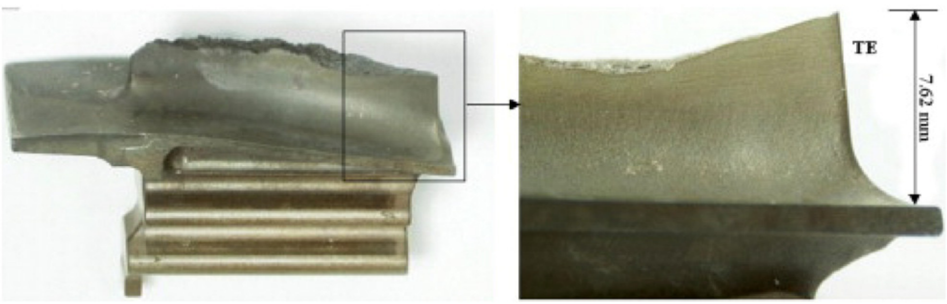

Fig. 18. View of the fractured blade [98].

Fig. 19. Fracture of the first four stage blades [106].

2003, on the premise of regarding aerodynamic loads on the inlet and outlet of impeller as the forces on the nodes, J. A. Kenyon et al. [119] analyzed the stress distribution of an impeller. In 2005, Luo et al. [120] conducted a modal analysis for a micro-gas turbine impeller, and the effects of prestress, centrifugal force stiffening, and rotation softening on the impeller modal were involved in the calculation. In 2008, Tang et al. [121] studied the stress distribution of a double suction impeller, and the effects of flow field pressure on the structural stress were involved. In 2008, Wang [122] simulated the whole flow field including the intake chamber, the intake guide blade, the first stage impeller, and the diffuser without blades for blade fracture of a first stage compressor impeller, and found that vibration fatigue of the impeller blade was due to pressure pulsation caused by the rotating stall. In 2008, Liu [123] analyzed the rotating stall of a large centrifugal compressor welding impeller, and fatigue seemed to be due to the superposition of stress caused by the rotating stall and other stresses.

For turbomachines working at high temperatures such as steam turbines, gas turbines, and aero-engine turbines, mechanical analysis of I&B should involves the effects of temperature. In 2008, Peng [124] analyzed the stress and strain of a blade in a large gas turbine under a centrifugal load, aerodynamic load, and temperature load. He found that there was a high stress area at the blade root and the maximum stress appeared at the root of the blade suction surface. In 2010, Duan [125] obtained the distribution of stress and strain of an aero-engine impeller under a centrifugal load and temperature load through the finite element method in which the linear elastic model of material was used by finite element software PATRAN and NASTRAN. In 2011, Li et al. [126] computed the stress of a composite impeller in the chiller, and aerodynamic load, blade weight, centrifugal load, and temperature load were involved in the calculation. The results showed that centrifugal load was the main alternating load in the open/stop stage, aerodynamic load was the major alternating load, and centrifugal load was nearly constant in the steady operation stage. In 2012, Li [127] conducted a thermal-structure coupling calculation by the sequential coupling method, and centrifugal load, thermal load, and aerodynamic load were involved in the calculation. On the premise of regarding the calculated temperature distribution as the temperature boundary condition, the thermal stress of an impeller was obtained. In addition, on the premise of regarding aerodynamic loads on the inlet and outlet of the impeller as the forces on nodes, the stress distribution of an impeller under aerodynamic loads was obtained. The results showed that the stress and the displacement of an impeller decrease when aerodynamic load is involved in the calculation because the direction of aerodynamic load is vertical to the direction of centrifugal load.

Through relevant mechanical analyses of I&B, preliminary conclusions of fatigue failure have been obtained. In 2001, Zhu [128] analyzed dynamic stress and fatigue life of last stage 668 mm-all-connected-blades in a 200 MW steam turbine under variable loads through the finite element method and relevant tests. In 2002, Xie et al. [129] established a fatigue life prediction model of turbine blades according to the analysis of dynamic stress, the Neuber guideline, and the rain-flow counting method. Various factors affecting failures of turbine blades were involved. In 2006, Fu [130] computed the cyclic stress of disk, blade, and tenon/mortise in each flight state and found the dangerous position of fatigue fracture in the key components, which were based on the thermal elastic–plastic finite element method and the contact nonlinear finite element analysis theory. In 2009, Lin [131] conducted a transient analysis and obtained the stress response after establishing the finite element model of a blade and applying the boundary condition. The high stress area and the danger position of fatigue failure determined by numerical analyses were consistent with that of actual blades under working conditions. In 2012, E. Poursaeidi [132] analyzed static stress and dynamic stress on a three-dimensional model of blade and disk by ANSYS. The result showed that cracks initiated from the high stress area under the actions of static force and dynamic force. In addition, the resonance under the first and the second order natural frequency was the major reason of blade fatigue which was judged by the result of the Campbell diagram analysis.

From a large number of numerical analyses, it has been found that the forced vibration of a blade caused by an aerodynamic load is a small part of the alternating load of I&B under steady operating conditions, and even the forced vibration may optimize the stress distribution of the blade. Therefore, the resonance caused by an aerodynamic load seems to be the cause of I&B fatigue. In recent years, many vibration fatigue accidents of large centrifugal compressor impellers have generally been because of vibration mode localization, and relevant scholars [133] concluded that the most important cause of I&B fatigue failure under steady operating conditions was the mistuning of the impeller. The mistuning of the impeller may result in vibration mode localization of the impeller. The local resonance of the impeller may occur when the frequency of the aerodynamic load falls into the natural frequency range of impeller vibration mode localization. The local resonance finally results in fatigue failure of the impeller. The

Table 1
Some resumes of fatigue failures.

No.	Name of elements	Failure mechanism	Crack initiation zone	Main cause of failures
I-1	The first stage SNCM 5 impeller	High cycle fatigue	Thin walls of rivet holes	The change of working conditions
I-2	An nitric oxide centrifugal compressor AISI410 impeller	High cycle fatigue	The inlet blade root	Fastening bolt with improper material
I-3	A first stage impeller in a X4CrNi13-4 air compressor	High cycle fatigue	The blade root	The unstable transient operation
I-4	The third to the fifth stage of a copper-based brazing impeller	High cycle fatigue	The brazing seam	Defects and composition segregation area caused by the brazing
I-5	The first and the second stage 34CrNi3Mo impellers	High cycle fatigue	Welding heat affected zone	Welding craters
I-6	A second stage impeller	High cycle fatigue	The joint of blade and disc	Abnormal microstructure
I-7	A first stage impeller	High cycle fatigue	The blade pressure surface	FOD
I-8	The first stage impeller in an air compressor	High cycle fatigue	The blade root	Metallurgical defect and hot processing defect
I-9	The H240-9.5/0.98 centrifugal compressor impeller	High cycle fatigue	The blade root	Vibration caused by design defect
I-10	The DHP56-1 centrifugal compressor blades	High cycle fatigue	The blade root	Work in the resonance region
I-11	A centrifugal compressor impeller	Corrosion fatigue	Welding seam at blade root	The corrosion of hydrogen sulfide
I-12	The second stage impeller in a HLR806-2 centrifugal compressor	High cycle fatigue	The blade tip	Vibration caused by the scale layer on the local blade surface
II-1	The first stage blade	High cycle fatigue	The blade profile bottom	The blade resonance caused by the low frequency excitation force
II-2	The first stage blades in a AG060/14L5 axial–centrifugal multiplex compressor	High cycle fatigue	Corrosion pits at blade root	Corrosion; operation under low flow
II-3	A Z1600-0.245/0.0961 axial compressor blade	High cycle fatigue	The blade root	The blade resonance
II-4	The ninth stage impeller in an axial air compressor	High cycle fatigue	The transition arc at the blade root	Complex alternating stress
III-1	A synthesis gas compressor turbine	High cycle fatigue	The blade root	Large alternating bending stress
III-2	A tenth stage blade in a FCC25-3.43/2.0/0.9 steam turbine	High cycle fatigue	The blade trailing edge	The abnormal vibration
III-3	A generator rotor turbine fan blade	High cycle fatigue	The airfoil root	The unsteady aerodynamic force
III-4	A fourth stage blade in a low pressure steam turbine	Corrosion fatigue	Corrosion pits on the blade leading edge	Vibration; a small leak of seawater in the condenser tube
III-5	A steam turbine in a KT1202 air compressor	Corrosion fatigue	Corrosion pits on the blade pressure surface	Corrosion
III-6	A fourteenth stage blade	Corrosion fatigue	The blade root	The uneven distribution of Cr
III-7	A second to last stage blade in a N200-130/535/535 steam turbine	Corrosion fatigue	Corrosion pits on the blade trailing edge	Cl corrosion
III-8	A low pressure turbine blade in a thermal power plant	Corrosion fatigue	The aerofoil region, 113 mm from the root	Cl corrosion; the impingement of silica particles
III-9	A last stage blade	Fatigue; stress corrosion cracking	The corner of the blade leading edge	S and Cl corrosion
III-10	The last stage blades in a N135-13.24/535/535 135 MW steam turbine	Corrosion fatigue; stress corrosion	The salient near the blade leading edge	Complex stress; chemical corrosion
III-11	A last stage blade	High cycle fatigue	The salient of blade suction side	Vibration
III-12	A turbine blade in a thermal power plant	High cycle fatigue	A pit on the blade trailing edge	Water erosion
III-13	A last stage blade	High cycle fatigue	The blade root	Large alternating stress
III-14	The last stage steam turbine blades	High cycle fatigue	The blade trailing edge root	Operate below the design condition
III-15	A first stage blade	Low cycle fatigue	The secure pinhole at the blade root	Excessive thermal stress
IV-1	A first stage blade in a YLII-7000A double-stage flue gas turbine	Corrosion fatigue	The location of blade near mortise	S corrosion; the high local stress
IV-2	A flue gas turbine blade	High cycle fatigue	The blade tenon	The uneven contact between tenon and mortise; vibration
IV-3	The first stage blades in a YLII-10,000 K flue gas turbine	High cycle fatigue	The blade tenon	Stress concentration caused by tenon and mortise; uneven microstructure
IV-4	The first stage blade in a TP3142/2.36-1.146 gas turbine	High cycle fatigue	The blade tenon	The bad assembly between tenon and mortise
IV-5	A flue gas turbine blade	High cycle fatigue	The blade tenon	The bad assembly between tenon and mortise; over temperature
IV-6	A flue gas turbine blade	Fretting fatigue	The blade tenon	The bad assembly between tenon and mortise
V-1	A fourth stage blade	High cycle fatigue	The blade trailing edge	Vibration; corrosion
V-2	A first stage blade	High cycle fatigue	The abrasion position on the blade suction surface	The improper angle of the zero order adjustable blade
V-3	The first stage compressor blades	Low cycle fatigue	Corrosion pit on the blade pressure surface	Flutter
V-4	A blade at the front row rectifier	High cycle fatigue	The blade leading edge	Vibration; abnormal microstructure

(continued on next page)

Table 1 *(continued)*

No.	Name of elements	Failure mechanism	Crack initiation zone	Main cause of failures
V-5	The first stage blades	High cycle fatigue	The blade root	The first order bending vibration
V-6	The third stage blades	High cycle fatigue	Pits on blade leading edge	Vibration; S and Cl corrosion
V-7	A single stage compressor	High cycle fatigue	The blade root	A forging defect
V-8	A fifth stage blade	High cycle fatigue	The blade leading edge	Material defect; vibration
V-9	A helicopter engine compressor blade	High cycle fatigue	A pit on blade leading edge	Corrosion; vibration
V-10	A first stage blade	Low cycle fatigue	Fretting marks on the tenon/mortise	The improper clearance between tenon and mortise
V-11	The 15th to 17th stage blades in a J79 engine compressor	Low cycle fatigue	Multiple origins	Serious rotating stall
VI-1	The third stage blades	Creep fatigue; high cycle fatigue	The blade tenon	Large clearance of adjacent blades; insufficient material property
VI-2	The third stage turbine blades	High cycle fatigue	The blade tenon	Vibration stress
VI-3	A low pressure turbine blade	High cycle fatigue	The transition arc of the blade coating	Excessive bending vibration
VI-4	The third stage turbine blades	Creep fatigue; complex fatigue	The blade tenon	Large clearance of neighboring shrouds
VI-5	A second stage turbine blade in a fighter	Creep; low cycle fatigue	The blade root	Abnormally high stress at elevated temperature
VI-6	The J69-T-25 turbojet engine turbine blades	High cycle fatigue	A position of surface friction	Excessive heat damage; eccentricity of shaft
VI-7	The aero-engine high pressure turbine blades	Thermo-mechanical fatigue	A cooling hole	Inadequate microstructure
VI-8	Two high pressure turbine blades	Hot corrosion; high cycle fatigue	The blade tips	The high temperature led to microstructure deterioration
VI-9	The second stage turbine blades	High cycle fatigue	Stress concentration position	Surface recrystallization; uneven microstructure
VI-10	Two blades in an aero-engine	High cycle fatigue	Near the blade trailing edge	Recrystallization
VI-11	A third stage turbine blade of a turbojet engine	High cycle fatigue	The blade root	Improper manufacturing process caused the separation of Ti and Mo
VI-12	The last stage blade in an aircraft gas turbine	High cycle fatigue	The blade trailing edge	The pores and segregation area of hafnium and titanium
VI-13	A fourth stage blade in a helicopter engine turbine	High cycle fatigue	A corrosion pit at the blade root	Corrosion; cyclic loading
VI-14	A blade in an aero-engine	High cycle fatigue	The blade root	Large local stress; fretting
VI-15	The second stage gas produce turbine	High cycle fatigue	The blade root	Large precipitate particles
VI-16	A single crystal blade	High cycle fatigue	The blade trailing edge	Excessive stress; the friction between blade tip and engine casing
VI-17	A first stage blade	High cycle fatigue	The blade trailing edge	Material defects
VII-1	A first stage turbine blade	Thermo-mechanical fatigue	Near the blade root	The design defects
VII-2	A second stage turbine blade	Low cycle fatigue	The blade tenon	Excessive stress; over temperature
VII-3	A first stage turbine blade	High cycle fatigue	The blade root	Resonance
VII-4	The low pressure compressor blades	High cycle fatigue	The blade tenon	The bad assembly of disk and blade
VII-5	A first stage turbine blade	Low cycle fatigue	Near the blade root	Particle erosion; alternating stress

Note: I — the centrifugal compressor, II — the axial compressor, III — the steam turbine, IV — the flue gas turbine, V — the aero-engine compressor, VI — the aero-engine turbine, and VII — the gas turbine.

mistuning of impellers seem inevitable in the machining and service of impellers, so mechanical analysis of the mistuned impeller is necessary for the determination of fatigue loads.

3.2. Vibration mode localization of impellers

The study of vibration mode localization mostly focuses on the one-dimensional linear periodic structure, the two-dimensional periodic structure, and the cycle periodic symmetric structure such as the blade–disk [134,135]. For the problem of vibration mode localization, quantitative numerical analysis needs to be further developed [136,137]. The vibration mode localization mechanism of the simple periodic structure has been intensely studied, but research on vibration mode localization of cycle periodic symmetry structures such as the centrifugal impeller which is combined with shroud–blade–disk is in the beginning stage.

In the design and machining of I&B, we try to avoid the resonance of I&B in operation. However, the mistuning of the impeller is inevitable due to the machining, running, and other reasons, and a small mistuning can lead to a large change of the impeller modal. The local resonance of the impeller may appear and result in fatigue failure of the impeller when the frequency of the aerodynamic load falls into the natural frequency range of the impeller vibration mode localization [133,138,139].

In 1988, S. T. Wei et al. [140,141] first solved the natural frequencies and the modal shapes of the mistuned blade–disk by a combination of the corrected perturbation method and the modal analysis method, and studied the steady response of the structure and the vibration mode localization. In 1992, C. Pierre et al. [142] analyzed the vibration mode localization of the mistuned blade–disk by the perturbation method. In 1995, B. C. Watson et al. [143] systematically studied the mechanical characteristics of the mistuned cycle periodic structure such as the blade–disk, and the concept of the mistuned modal was introduced to describe the mistuning of the structure. In 2000, T. Krzyzynski et al. [144] simulated a blade using a linear Euler–Bernoulli beam model, and the effects of blade damping on the vibration mode localization were studied. In 2003, H. H. Yoo et al. [145] studied the vibration mode localization of the mistuned cycle structure under a harmonic force using a simplified cycle periodic structure model, and the results showed that the effects of mistuning, coupling, and damping result in vibration mode localization. Zhou et al. [146,147] solved the vibration mode localization problem of a mistuned blade–disk using the finite element general program and modal analysis technique, and proved that the model and the numerical method were applicable to practical problems. In 2007, Li et al. [138] studied the dynamic characteristics and the steady response of a centrifugal compressor impeller under fluid excitation and estimated the impeller fatigue life according to the results of frequency response, and the fluid excitation resulted in the local resonance of the impeller. In 2008, Mao et al. [139] computed the first fourteenth order modals of a centrifugal compressor impeller blade and the static stress of a blade under centrifugal load using the finite element method, and they computed the equivalent alternating stress of a blade under unsteady aerodynamic loads using the one way fluid–solid coupling method. The results showed that local resonance appears in the area near the leading edge, and the large equivalent stress in this area results in high cycle fatigue of the blade. In 2009, Ding [148] conducted resonance analysis and harmonic response analysis of a cracked aero-engine blade, and studied the change of the blade harmonic response caused by the crack. The amplitude of harmonic response increased with the increase of crack depth when the crack was in the same position. The amplitude of the harmonic response decreased with an increase of the distance between the location of the crack and the blade root when the crack depth was constant. The crack also changed the phase of blade response. In 2012, Zhao et al. [133] studied vibration mode localization of a large centrifugal impeller. They pointed out that vibration spread throughout whole structure when the excitation frequency was in the "frequency pass band", and the vibration amplitude and energy were mainly confined within a local area when the excitation frequency was in the "frequency forbid band". Numerical analyses showed that a large vibration amplitude appeared on the blade inlet which was consistent with the actual failure position of the impeller when the excitation frequency was close to the "frequency forbid band".

3.3. Numerical simulations of fatigue crack growth in the I&B

Numerical simulation of fatigue crack growth in I&B is a complex problem and has not been widely described in the literature. The stress intensity factor K is one of the most important parameter in fracture mechanics, which can be computed using the FEM or BEM [149].

The meshes are distorted in the numerical simulation of fatigue crack growth by the FEM. It is necessary to refine meshes near the crack tip and re-meshing in each step of crack growth, and which consume a lot of pre-processing time. In 2005, Hutson et al. [150] confirmed the efficacy of a fracture mechanics method to model the fretting fatigue cracks growth under test conditions similar to those found in turbine engine blade attachments, and the crack propagation lives were calculated using stress analysis results of the FEM. In 2009, Hu [151] calculated fracture mechanics parameters of an aero-engine turbine disk such as K, J integral and further simulated crack growth by FEM. A relation between the parameters and crack length was obtained and used to determine critical crack length. In 2012, Mohammad Rahim Nami [152] studied the mixed mode fracture induced by a semi-elliptical surface crack lying at the stress concentration zone of a rotating impeller under general loading condition. Different values of the crack geometrical parameters were considered. The problem of rapid changes in the geometrical parameters in the vicinity of the crack front, which needs to incorporate very high mesh density, was solved by applying the submodeling technique. The calculated Ks in the mixed mode were reasonable and could be used to predict the crack growth rates. The distributions of Ks along the crack front were studied and the effects of the aspect ratio and relative depth of the crack were investigated. In 2014, Gao et al. [153] analyzed the crack characteristics in the tenon of nickel-based single crystal superalloy turbine blade by a rate-dependent crystal slip finite element program, and the influence of crystallographic orientations was also taken into account. The Mises stress distributions of the crack tip in the tenon under an isotropic condition combined with different crystal orientations were studied, and the crack propagation trend was examined. In 2014, Liu [154] analyzed the fatigue crack propagation base on the 2D simplified model of the impeller contact surface with through-thickness cracks in different locations, and the Ks of the cracks in different locations and different working conditions were calculated by the J-integral method. The crack growth rate and the residual life of the cracks under different rotational speeds were computed by the Paris model. The computations made a contribution to the determination of the critical threshold of impeller remanufacturing. In 2014, Witek [155] presented results of crack growth analysis of an aero-engine compressor blade subjected to resonant vibration. An original hybrid method was used for crack dynamic estimation. The proposed procedure connects three methods: analytical, numerical and experimental fatigue analysis of the blade tested in high cycle fatigue conditions. During investigations only the first mode of transverse vibration was considered. The K for the simplified blade model with a half-elliptical crack was calculated using the Raju–Newman method. The bending stress used in the Raju–Newman solution was computed for the real blade model by the FEM, and K values were substituted into the Paris–Erdogan equation. Simulation results were compared with the experimental crack growth analysis results performed for the first stage compressor blade of a helicopter turbo-engine.

The boundary of solution domain is divided and the function meeting control equations approaches the boundary condition in the BEM. Compared with the FEM, the calculation accuracy of the BEM is greatly improved, which is more suitable to deal with the crack problem. In addition, the BEM significantly reduces the computing time. However, the BEM is still a numerical simulation method base on mesh, and meshes are revised in the crack growth simulation. In 2005, K. W. Barlow [156] computed the 3D fatigue crack growth rates in a typical military aircraft engine fan blade attachment under centrifugal and aerodynamic loads. The crack growth simulations utilized FRANC3D, which uses boundary elements and linear elastic fracture mechanics. The displacements and *K*s were calculated on the crack's leading edge to yield crack propagation trajectories and rates. The simulations indicate a strong interaction between K_{I} and K_{III} at the contact edge. E. Poursaeidi did a lot of works on the numerical simulation of crack growth in I&B by BEM. In 2007, E. Poursaeidi [47] evaluated *K*s along 3D crack fronts by the FRANC3D. The calculated *K*s indicated that K_{I} plays a strong role in propagation, and this is due to that the stresses were perpendicular to the crack area. The research also indicated that the average *K* along the crack front exceeds the critical *K* and ductile fracture could occur. In 2009, E. Poursaeidi [157] simulated crack propagation and further predicted the fatigue life of the blades. The displacements and *K*s were computed on the crack near the leading edge to calculate crack propagation trajectories and rate. The modified Paris model and Forman–Newman–de Koning (FNK) model have been used to estimate the fatigue crack growth rate. In 2014, E. Poursaeidi [158] conducted analyses of static and dynamic stress by Abaqus software. In addition, the fracture mechanics criterion was used to simulate fatigue crack growth using Franc3D. First, *K*s for one semi-elliptical surface crack and then *K*s for two semi-elliptical surface cracks were taken into account. Second, the Paris and FNK models were used to predict fatigue life. *K*s results indicated that insertion of a second crack has no effect on the final *K*, however, the second crack facilitates the process of reaching the critical length. Witek also did much work in this area by the BEM. In 2011, Witek [159] used a dual boundary element method to calculate *K* of a semi-elliptical crack in blades. In 2014, Witek [149] presented results of numerical crack propagation analysis of compressor blades subjected to transverse vibrations. For *K* calculation in the half-elliptical crack, a dual boundary element method was used. Simulation results were compared with experimental results of PZL-10W engine compressor blades tested in resonance conditions.

The XFEM overcomes the difficulty of high mesh density in the high stress and strain concentration area such as the crack tip, and re-meshing in the crack growth simulation is not needed for the XFEM. But the XFEM is more complex than the FEM in the computation of the element stiffness matrix, and this problem is more prominent in 3D cases. In addition, the freedom degree of node and scale of overall equations are increased because of the introduction of the discontinuous displacement field and singular displacement field. In 2014, Matthias Holl et al. [160] proposed a new multiscale technique to investigate advancing cracks. This technique is designed to efficiently take into account cracks of different length scales, by locally enabling fine scale domains in regions of stress concentrations and high stress gradients. Cracks are modeled using the XFEM, which invokes the partition of the unity method, combined with the level set method (LSM), and allows us to follow the advancing crack fronts independent of the finite element mesh. The J-integral yields an accurate solution of the *K*s, and with the criterion of maximum hoop stress, a precise direction of growth. Once the most damaged quadrature point in the gas turbine blade is localized, the proposed crack propagation model is applied, to determine the crack growth at the microscale.

3.4. Summary of numerical simulations of the I&B fatigue

The I&B in service suffer complex loads such as the centrifugal load, the aerodynamic load, the temperature load, and the vibration load. Also, the I&B are affected by the service history. So it is difficult to obtain the accurate fatigue load, or the load spectrum. In fact, the contributions of some loads to fatigue failure of I&B are extremely small. Therefore, we can determine the main loads which lead to the fatigue failure of I&B according to the service characteristics of different turbomachines. The relevant analyses of main loads are conducted through the finite element method. Then we can obtain the preliminary conclusions of fatigue load and fatigue failure of I&B.

The vibration mode localization of impellers usually leads to fatigue failure of I&B. For an impeller with periodic structures, slight mistuning can lead to a large change of impeller dynamics, and the mistuning of the impeller is almost unavoidable in reality. The relevant dynamic analyses of a mistuned impeller are necessary for the determination of fatigue load. Also, the quantitative numerical analysis of vibration mode localization of I&B needs to be further developed. The statistics of typical mistuning of I&B, the perfect analysis method for the mistuning response, the fast multi-parameter calculation method for mistuning sensitivity, the standards of the natural frequency and the dynamic strength of a mistuned impeller are rare in engineering. So we need to introduce a nominal equivalent mistuning parameter to characterize the degree of mistuning, and build a relationship of dynamic response after mistuning with the equivalent mistuning parameter. By measuring each order's natural frequency of mistuned I&B and comparing them with an ideal impeller, we can determine the extent of mistuning, and then estimate the stress distribution in order to repair the I&B and avoid strength fracture or the fatigue of I&B in operation.

Although the numerical simulations of fatigue crack growth reduce a lot of experiment costs, there is little literature about numerical simulations of fatigue crack growth in I&B because of the lack of fatigue crack growth rate equations for specific materials under different loads, the difficulty of establishment of 3D finite element model of I&B particularly the crack model, the immaturity of fatigue crack growth theory, the uncertainty of fatigue crack growth direction under multiaxial loads, and other reasons. Currently, the FEM, BEM, and XFEM have been applied in numerical simulations of fatigue crack growth in I&B. The application of the FEM and BEM are more common, but are restricted by meshing technology. The meshless method which is based on the discrete node to obtain the interpolation function, has a great advantage in the dynamic simulation of crack growth. But the meshless method has not been applied in the numerical simulation of fatigue crack growth in I&B. In addition, the meshless method greatly increases the computing time. The coupling of the discretizing crack tip region by the meshless method and in the remaining area by the FEM can harmonically improve the simulation precision and efficiency.

4. Fatigue tests of the I&B

Fatigue tests are the basis of intensive research on fatigue behavior and mechanism of I&B. The most important issue in fatigue tests of I&B is how to realize the accurate simulation of complex loads. Current fatigue tests of I&B mostly focus on the aero-engine blade, and there are relatively fewer fatigue tests of centrifugal compressor impellers.

The key point of fatigue tests of I&B is the simulation of fatigue load in the assessment position, especially for the stress field and the temperature field. The low cycle centrifugal load is usually equivalent to the pull–pull load. The lever weight loading, the hydraulic servo loading, and the electromechanical servo loading are the most important loading methods [161]. Yan et al. [162] mounted an impeller on a high speed spindle, and simulated the centrifugal load through spindle turning. Vibration load is the main reason for I&B failure. The pulses gas excitation, beam electromagnetic excitation and the moving coil electromagnetic excitation are the main methods to provide vibration load. The electromagnetic vibration table and the vibration exciter are the most important devices for high cycle fatigue tests of I&B. The temperature load is provided by electric heating, and the high temperature environment is usually simulated by the uniform temperature field in the assessment section. Isothermal simulation cannot produce the thermal stress caused by the temperature gradient, so the thermal stress is replaced by the appropriate increase of load in the test. The heat furnace which is used in the simulation of high temperature environments of I&B usually includes the resistance furnace, the high-frequency induction furnace, and the vacuum furnace. The resistance furnace is usually used in high temperature fatigue tests of standard specimens because of the convenience of use and good uniformity of the temperature field. The heating of local I&B, the fast speed of heating and cooling, and the convenience of observation are the main advantages of the high-frequency induction furnace. However, it is only suitable for heating of ferromagnetic material, and the heating effect is poor for weak ferromagnetism material and non-ferromagnetic material. The vacuum furnace is usually used in higher temperature fatigue tests (e.g. 2000 °C which is the upper temperature limit of a vacuum furnace at Texas A&M University [163]) to prevent the oxidation of the specimen. The thermocouple, the measurement of the exhaust temperature, and the thermal point are the main methods of measuring the temperature field of I&B. For example, Wang et al. [164–166] established a thermo-mechanical fatigue test system of blades which was based on high-frequency induction heating equipment, and conducted relevant thermo-mechanical fatigue tests of the test device as shown in Fig. 20.

A special fixture is needed to ensure that the stress in the assessment position is the same or close to the actual stress of the blade. The simulation of the stress field is verified through the calibration of the stress field and fracture analysis. The fixture at high temperature which simultaneously provides the axial tensile load and the bending moment to the I&B with complex geometries faces the following difficulties: the fixture should simultaneously provide the tensile load and the bending moment, the magnitude of bending moment should be adjustable, the blade material in and near the assessment position should be undamaged and unchanged, the fixture at high temperatures should have sufficient strength and clamping force, and the fixture cannot affects the loading system of the test machine.

Fatigue tests of I&B are divided into three types according to the specimen: the standard specimen fatigue test, simulation specimen fatigue test, and actual I&B fatigue test [163]. The fatigue life data of blade material in the service environment are

Fig. 20. Thermo-mechanical fatigue test system for blades [164].

obtained by the standard specimen fatigue test. The standard specimen fatigue test has the advantages of the simple shape of the specimen and the convenience of loading and stress–strain description. In addition, the standard specimen fatigue test results are beneficial to the establishments of the basic constitutive relation and fatigue damage model. However, the test results of standard specimens are very different from I&B because the material properties and the stress states of I&B with complex geometries and various molding processes are different from that of standard specimens. The design of the simulation specimen which represents the typical geometry, processing techniques, stress, and other characteristics of I&B is the first step of the simulation specimen fatigue test. Nie et al. [163] studied the differences of fatigue life at different locations of a directionally solidified turbine blade using the simulation specimens of blade tips shroud, blade, platform, and tenon. The European PREMECCY program [167] and the relevant research on the fatigue life of turbine blades in Germany also involved simulation specimens [12]. Compared with the I&B fatigue test, the simulation specimen fatigue test has the advantages of easy loading and convenient testing. Also, the results of the simulation specimen fatigue test are beneficial to theoretical modeling and the increase of prediction accuracy of the life model. But there are some differences between the simulation specimens and the actual I&B such as the geometry, processing techniques, and stress state. In addition, the design of simulation specimens is difficult. The difficulties of actual I&B fatigue tests are different. The high cycle fatigue test of a blade can be conducted by a vibration table, but the tests of multiaxial fatigue and combined fatigue are more complex. The actual I&B fatigue test is the development direction and the research focus of the future, and the technical difficulty is the accurate simulations of load and service environment of I&B. Complete research information in this area has not been produced.

4.1. Vibration fatigue tests of the I&B

Vibration fatigue is the main method of I&B fatigue tests. In 1984, Gao et al. [168] conducted fatigue tests of specimens which suffered different anti-water erosion processes using a 10 kW beam vibration fatigue test table. The plate specimen was equivalent to the straight blade with uniform section, and the holder section and the test section were equivalent to the blade root and the blade profile, respectively.

The fatigue testing system is the basis of I&B fatigue tests. In 1985, Lu [169] proposed a new fatigue testing system with closed-loop control, which significantly improved the accuracy of the loading system and basically realized the automation of the vibration fatigue test. In 1987, Xu [170] developed a new type of blade vibration fatigue tester according to the principle of the electromagnetic eddy current. The excitation force was directly applied on the specimen, and the position of excitation point was adjustable. The test capability of high mode vibration fatigue of this equipment was powerful. In 1988, Hou et al. [171] studied the vibration fatigue characteristics of the third stage TC11 titanium alloy blade in a turbojet engine compressor and the blade material by the vibration fatigue method. In 1990, Sun et al. [172] studied the fatigue life of blades whose leading edge had pits caused by FOD using test equipment which included the excitation system and the test system. The vibration amplitude of the blade tip was monitored by a reading microscope, camera, and closed circuit television, and the blades were tested under the resonance condition of the first order bending mode. In 1998, Kang et al. [173] tested the remaining vibration fatigue life of TC4 plate blades with pits caused by FOD using the vibration fatigue test system which was established according to the electromagnetic eddy current excitation principle. Cai et al. [174–179] studied the fatigue behaviors of relevant blades using the vibration fatigue test method. In 2005, Zhang et al. [180] proposed a new method for the vibration fatigue test of blades at high temperature through the combination of electronic induction heating and electromagnetic vibration table. In 2006, Ge [181] developed a blade vibration fatigue testing device to simulate the forced vibration of a blade by an eccentric wheel, and tested the fatigue limit of 2Cr12MoV turbine blades with three surface treatment states by the small sub-sample lift and drop method. In 2009, Shao et al. [182] proposed a vibration fatigue testing method with high frequency, and the inertia load with a fixed frequency on the specimen was applied by the vibration table and a rigid mass block. The vibration fatigue test with high frequency around 1000 Hz was carried out under a symmetrical load. L. Witek [159,183,184] conducted vibration tests of blades in a helicopter engine. The device is shown in Fig. 21. The blades were retired and included two kinds, i.e. with and without stress

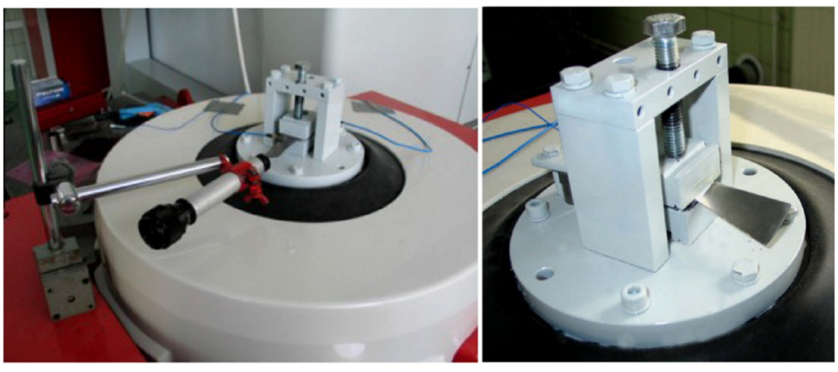

(a) View of the test device (b) View of the specimen

Fig. 21. Blade vibration fatigue test device [183].

concentration. The tests were conducted under the resonance condition of lateral vibration and the propagation of crack was monitored. In addition, the blade vibration stress was computed by the nonlinear finite element method when the first mode transverse vibration of the blade occurred. The crack initiated from the position of the maximum principal stress. In 2011, Li et al. [185] conducted the first mode bending vibration fatigue tests of aero-engine compressor blades at room temperature by the ES-50 electromagnetic vibration table, and determined the blade vibration fatigue limit at 10^7 cycles. The fatigue life analysis showed that the Basquin equation predicted the blade vibration fatigue life as well at lower vibration stress and also at higher vibration stress when the Basquin equation was corrected by introducing a new strain ratio factor. In 2012, Li et al. [186] developed a cantilever bending vibration ultrasonic fatigue test system. The system can simulates blade vibration through the special specimen and is suitable for the bending vibration fatigue tests in a very high cycle regime. The bend vibration fatigue tests of titanium alloy TC17 in the very high cycle regime were carried out by this system. In 2013, Wang [187] invented a vibration fatigue test device for the whole impeller. A rubber damper was placed in the clearance of adjacent blades, so the other blades cannot freely vibrate when the vibration fatigue test of one blade was conducted. This method not only avoids the trouble of cutting the whole impeller, but also avoids the change of blade natural frequency because of the stiffness change of the disk, and which ensures the reliability of vibration fatigue test results.

4.2. Combined fatigue tests of I&B

The I&B in service not only suffer centrifugal load, aerodynamic load, and temperature load with large amplitude and low frequency, but also suffer vibration load with small amplitude and high frequency. When vibration load and low cycle load simultaneously act on the I&B, it is a combined fatigue problem which is different from low cycle fatigue and high cycle fatigue. Research on combined fatigue of I&B faces important difficulties as follows: simulation of the superposition of low cycle load and high cycle load, determination of high cycle load, and theoretical prediction of the combined fatigue life [163].

In recent years, many studies on the test methods of multiaxial fatigue have been conducted such as the simulation of multiaxial load by the shape change of a specimen under uniaxial load. A new generation of electro-hydraulic servo multiaxial fatigue test machines can simulate complex loads of several components in service such as the combination of tension and torsion, and which powerfully supports the study of multiaxial fatigue. Multiaxial fatigue test researches on I&B are imperfect at present. In the early stage of multiaxial fatigue test researches on blade material, the shapes of specimens were usually the crisscross pattern or the thin wall tubular, and which were very different from the actual blades. Up to now, relevant scholars have conducted some combined fatigue tests of aero-engine blades and blade material.

In 1992, Xu et al. [188] developed a combined fatigue test machine to simulate the actual loads of a blade, and conducted a series combined fatigue tests under different loads and different frequencies with this machine. This fatigue test machine provides the combined load of tension and bend. The low cycle load is the pulsating tension provided by a hydraulic actuator and the high cycle load is the bending vibration which is vertical to the direction of the low cycle load and is provided by an eccentric shaft driven by a DC motor. The heating system works through electromagnetic induction with high frequency, and the cooling system works through the intermittent supply of water. Since 1996, Yan et al. [189–196] proposed a combined fatigue testing method for turbine blades and conducted relevant tests. The centrifugal load of the blade is simulated by the pulling force of a rod, the vibration load of the blade is provided by the electromagnetic vibration exciter, and the high temperature load of the assessment position is applied by the electromagnetic induction coil. The fixture overcomes the disadvantage of the easy slippage of the blade according to the rubbing principle. In 2000, NASA studied blade fatigue through a combined redesigned fixture and standard specimens [197]. In 2001, the Portugal Materials and Surface Engineering Research Institute proposed a new combined fatigue testing method [198]. Through installing an electronic exciter in a traditional fatigue test machine to simulate the blade vibration, a platform for the pull–bend fatigue test of plate specimen and rod specimen was established. The combined fatigue property of an engine blade was effectively tested by this method for the accurate simulation of blade load. In 2004, Xie et al. [199] developed a combined fatigue testing system for blades. The vibration load of bending or twisting is applied to the blade under the action of tension. The radial centrifugal load is provided by a large vibration exciter and the vibration loads are provided by two small vibration exciters on other axes. The magnitudes of bending load and torsion load are adjustable through the changes of angles of two small vibration exciters. In 2006, R. Rajasekaran et al. [9] conducted combined fatigue tests of blade tenon roots under the actions of tension and bending vibration. The fatigue loads of the compressor blade in service were simulated by this method, and the fatigue life predicted by the relevant model very well fit the test results. In 2011, B. W. Lee et al. [11] invented combined fatigue testing equipment to simulate centrifugal load and blade vibration. The fretting fatigue test of a tenon was conducted with this equipment, and the fatigue crack initiated from the contact edge. In 2014, Wang et al. [200] proposed a combined fatigue test method which was based on the vibration table and relevant fixtures. The fixtures were assembled on the vibration table to provide various loads such as tension, compression, bending moment, twisting moment, and a combination of above loads. The test frequency range of this method is 5–4500 Hz, and this method seems suitable for the combined fatigue tests of I&B.

4.3. Summary of I&B fatigue tests

The fatigue tests of standard specimen, simulation specimen, and actual I&B complement each other, and provide comprehensive test data for the theoretical prediction of fatigue life of I&B. The fatigue test of actual I&B has important significance for fatigue mechanism research and the fatigue life prediction of I&B for the actual I&B without any deviation of material property, geometry, and processing technique.

According to the service characteristics of I&B such as high excitation frequency, long service life, complex loads, and the great effects of the environmental medium, it is necessary to propose a new fatigue test method which is suitable for the fatigue test of I&B. Intense study of the fatigue of I&B which is based on the combined fatigue tests of I&B in a complex environment gives powerful supports to the design, use, safety assessment, and life prediction of I&B.

5. Conclusions

It can be concluded that:

(1) High cycle fatigue caused by vibration is the main failure mechanism of I&B. Fatigue failures of I&B are induced by the structure, material defect, processing techniques, corrosion, erosion, FOD, and other causes. Fatigue cracks usually initiate from the location of stress concentration. Fatigue failures of I&B can be prevented from aspects of design, material, manufacture, assembly, operation, and overhaul.
(2) The resonance caused by the aerodynamic load is the main cause of fatigue failure of I&B in a steady operating condition. The mistuning of the impeller caused by the processing technique or service may result in a change of impeller dynamic and vibration mode localization. The local resonance caused by vibration mode localization may leads to fatigue failure of I&B. The application of the FEM and BEM are more common than the XFEM in numerical simulations of fatigue crack growth in I&B, which is restricted by meshing technology. The coupling of the meshless method and the FEM is the development direction of the numerical simulations of fatigue crack growth in I&B.
(3) The fatigue tests of standard specimens, simulation specimens, and actual I&B complement each other, and provide comprehensive test data for the theoretical prediction of fatigue life of I&B. The vibration fatigue test and the combined fatigue test are the main methods of I&B fatigue tests. The combined fatigue test of actual I&B without any deviation of material property, geometry, and processing technique is the development direction and research focus of the future.

Acknowledgments

The authors gratefully acknowledge the financial support provided by the National Key Basic Research and Development Program (973 Program 2011CB013401). Thanks to Dr. Edward C. Mignot, Shandong University, for linguistic advice.

References

[1] J.H. Wang, Y. Qi, H. Su, J.S. Li, A summary of fatigue fracture in turbine blades, Turbine Technol. 06 (1999) 330–333.
[2] S.K. Bhaumik, T.A. Bhaskaran, R. Rangaraju, M.A. Venkataswamy, M.A. Parameswara, R.V. Krishnan, Failure of turbine rotor blisk of an aircraft engine, Eng. Fail. Anal. 9 (3) (2002) 287–301.
[3] N. Vardar, A. Ekerim, Failure analysis of gas turbine blades in a thermal power plant, Eng. Fail. Anal. 14 (4) (2007) 743–749.
[4] B. Zhang, Y.C. Li, A summary of failure analysis of blades in the Curtis stage and the second last stage of steam turbine, Turbine Technol. 02 (1990) 44–47.
[5] B.T. Zhu, The effects of the surface state of steam turbine blade on its fatigue life, Shanghai Turbine 01 (2000) 1–11.
[6] T. Kang, H. Wang, S.Q. Xi, M.X. Tong, J. Xiao, Fatigue behavior of high-frequency induction hardened blade steel, Heat Treat. Met. 02 (2012) 28–32.
[7] Z. Xu, J. Park, S. Ryu, Failure analysis and retrofit design of low pressure 1st stage blades for a steam turbine, Eng. Fail. Anal. 14 (4) (2007) 694–701.
[8] H. Tang, D. Cao, H. Yao, M. Xie, R. Duan, Fretting fatigue failure of an aero engine turbine blade, Eng. Fail. Anal. 16 (6) (2009) 2004–2008.
[9] R. Rajasekaran, D. Nowell, Fretting fatigue in dovetail blade roots: experiment and analysis, Tribol. Int. 39 (10) (2006) 1277–1285.
[10] Z. Mazur, A. Hernández-Rossette, R. García-Illescas, Investigation of the failure of the L-0 blades, Eng. Fail. Anal. 13 (8) (2006) 1338–1350.
[11] B.-W. Lee, J. Suh, H. Lee, T.-G. Kim, Investigations on fretting fatigue in aircraft engine compressor blade, Eng. Fail. Anal. 18 (7) (2011) 1900–1908.
[12] S. Issler, E. Roos, Numerical and experimental investigations into life assessment of blade–disc connections of gas turbines, Nucl. Eng. Des. 226 (2) (2003) 155–164.
[13] N. Isobe, S. Nogami, Micro-crack growth behavior and life in high temperature low cycle fatigue of blade root and disc joint for turbines, Int. J. Press. Vessel. Pip. 86 (9) (2009) 622–627.
[14] D.L. Davidson, Gas turbine disk–blade attachment crack, J. Fail. Anal. Prev. 5 (1) (2005) 55–71.
[15] Z.H. Dong, W. Lin, Failure analysis for impeller in air compressor, J. Hangzhou Inst. Electron. Eng. 03 (2000) 43–47.
[16] L.Y. Zhao, L.H. Zhang, L.H. Lin, Air compressor brazing impeller failure analysis, Phys. Test. Chem. Anal. A (Phys. Test.) 01 (1998) 31–33.
[17] C.R.F. Azevedo, A. Sinátora, Erosion-fatigue of steam turbine blades, Eng. Fail. Anal. 16 (7) (2009) 2290–2303.
[18] R. Ebara, Corrosion fatigue phenomena learned from failure analysis, Eng. Fail. Anal. 13 (3) (2006) 516–525.
[19] H. Kazempour-Liacy, M. Mehdizadeh, M. Akbari-Garakani, S. Abouali, Corrosion and fatigue failure analysis of a forced draft fan blade, Eng. Fail. Anal. 18 (4) (2011) 1193–1202.
[20] H. Kim, Y. Kang, Crack evaluation and subsequent solution of the last stage blade in a low-pressure steam turbine, Eng. Fail. Anal. 17 (6) (2010) 1397–1403.
[21] Z. Mazur, A. Luna-Ramírez, J.A. Juárez-Islas, A. Campos-Amezcua, Failure analysis of a gas turbine blade made of Inconel 738LC alloy, Eng. Fail. Anal. 12 (3) (2005) 474–486.
[22] E. Poursaeidi, M. Aieneravaie, M.R. Mohammadi, Failure analysis of a second stage blade in a gas turbine engine, Eng. Fail. Anal. 15 (8) (2008) 1111–1129.
[23] E. Poursaeidi, A. Babaei, F. Behrouzshad, M.R. Mohammadi Arhani, Failure analysis of an axial compressor first row rotating blades, Eng. Fail. Anal. 28 (0) (2013) 25–33.
[24] A.P. Tschiptschin, C.R.F. Azevedo, Failure analysis of turbo-blower blades, Eng. Fail. Anal. 12 (1) (2005) 49–59.
[25] J.M.B. Reeves, S.G. Lagrange, Some failure analyses of South African air force aircraft engine and airframe components, Eng. Fail. Anal. 5 (2) (1998) 105–112.
[26] I. Salam, A. Tauqir, A.Q. Khan, Creep-fatigue failure of an aero engine turbine blades, Eng. Fail. Anal. 9 (3) (2002) 335–347.
[27] E. Silveira, G. Atxaga, A.M. Irisarri, Failure analysis of a set of compressor blades, Eng. Fail. Anal. 15 (6) (2008) 666–674.
[28] G.S. Xie, Preparation and Related Basic Research of C_3N_4/TiN Composite Coatings Used in the Last-Stage Steam Turbine Blade for the Water Impact Erosion-Resistance(Doctor) Central South University, Chang Sha, 2008.
[29] B.A. Cowles, High cycle fatigue in aircraft gas turbines—an industry perspective, Int. J. Fatigue 20 (1) (1998) 82–83.
[30] Z.Z. Hu, N.S. Hu, Fracture analysis of a compressor impeller, J. Xi'an Jiaotong Univ. 04 (1986) 13–20.

[31] D.K. Cheng, The fracture reason analysis and repair of rotor blade in nitric oxide compressor, Compressor Blower Fan Technol. 04 (2007) (46-8 + 51).
[32] S. Sivaprasad, N. Narasaiah, S.K. Das, G. Das, S. Tarafder, K.K. Gupta, et al., Investigation on the failure of air compressor, Eng. Fail. Anal. 17 (1) (2010) 150–157.
[33] F. Hou, H. Xu, K.S. Guan, G.Q. Ye, Analysis on failure for cracking centrifugal compressor's impeller, Fluid Mach. 12 (2005) 36–39.
[34] Y.Q. Wang, Z.M. Wang, Fracture failure analysis for centrifugal compressor 2 step leaf wheel, Mod. Manuf. Eng. 01 (2006) 116–117.
[35] Z.M. Wang, E.F. Shang, S.H. Xue, Y.Q. Wang, A fracture failure analysis of the first stage impeller blade in vertical air compressor, China Academic Conference on Failure Analysis, Shanghai 2009, p. 4.
[36] L. Chen, J.M. Sun, H.H. Song, Fracture analysis on 1st stage impeller blade of main air compressor, Heat Treat. Met. S1 (2011) 59–63.
[37] X.L. Xiong, The accident reason and treatment measure of a centrifugal compressor impeller, Chem. Equip. Anticorros. 04 (2003) 23–24.
[38] W. Qi, The solution of a compressor blade fracture accident, Gen. Mach. 05 (2004) 64–67.
[39] S.Z. Hu, Analysis of cracking causes of impeller of rich gas compressor and countermeasure, Corros. Prot. Petrochem. Ind. S1 (2009) 63–68.
[40] X.M. Ma, L.X. Hu, Failure analysis on fracture of impeller blades of high-speed centrifugal aircompressor, Phys. Test. Chem. Anal. A (Phys. Test.) 08 (2011) (527-30 + 33).
[41] Y.P. Dai, J.L. Meng, L. Gao, Cause analysis of the rupture of the blades of the axial-flow compressors and their retrofit design, Chem. Eng. Mach. 01 (2006) 14–19.
[42] J.X. Xie, The cause analysis of fatigue for the first stage blade of axial-flow compressor, Compressor Blower Fan Technol. 02 (2007) 64–70.
[43] W. Fu, Reason analysis of blade cracking in catalytic cracking axial-flow compressor, Compressor Blower Fan Technol. 01 (2009) 63–65.
[44] J.H. Zhi, H.C. Zhang, Z.X. Lu, Y.F. Zhou, M.X. Liu, Failure analysis on blades in axial compressor, Fluid Mach. 02 (2011) 47–51.
[45] P.S. Zhang, C.Z. Deng, M.J. Tu, The fatigue fracture analysis of the blading material used on the French made KT-1501 steam turbine, J. Xi'an Jiaotong Univ. 04 (1985) 43–51.
[46] Z.X. Weng, Cause analysis of blade fracture in unit 4 steam turbine of Xiamen power plant, Guangdong Electr. Power 12 (2005) 69–71.
[47] E. Poursaeidi, M. Salavatian, Failure analysis of generator rotor fan blades, Eng. Fail. Anal. 14 (5) (2007) 851–860.
[48] H. Kim, Crack evaluation of the fourth stage blade in a low-pressure steam turbine, Eng. Fail. Anal. 18 (3) (2011) 907–913.
[49] H.T. Zhao, S.D. Wang, A fracture analysis of steam turbine blade in KT1202 air compressor, Petro-chem. Equip. Technol. 01 (1990) 43–46.
[50] F.L. Li, R.H. Zhu, S.Z. Cao, Z.Z. Hu, The multi-source fatigue fracture analysis of blade, Phys. Test. Chem. Anal. A (Phys. Test.) 04 (1997) (33-4 + 20).
[51] Z.F. Zhou, A fracture failure analysis of the second last stage blade in 200 MW steam turbine, North China Electr. Power 01 (1998) 56–57.
[52] G. Das, Chowdhury S. Ghosh, Ray A. Kumar, Das S. Kumar, Bhattacharya D. Kumar, Turbine blade failure in a thermal power plant, Eng. Fail. Anal. 10 (1) (2003) 85–91.
[53] Y.L. You, S.X. Rao, C.N. Chen, Z. Zhang, The fracture reason analysis of the last stage blade in steam turbine, Phys. Test. Chem. Anal. A (Phys. Test.) 41 (z1) (2005) 359–362.
[54] J.J. Chen, H.C. Zhang, G.C. Dai, Analysis of the cracks in the blades of low pressure stage of 135 MW steam turbine, Water Conserv. Electr. Power Mach. 04 (2007) 1–4.
[55] W.-Z. Wang, F.-Z. Xuan, K.-L. Zhu, S.-T. Tu, Failure analysis of the final stage blade in steam turbine, Eng. Fail. Anal. 14 (4) (2007) 632–641.
[56] S. Liu, Y.N. Zhao, Y.Z. Liu, Fracture reason analysis of last stage blade of 200 MW steam turbine, Turbine Technol. 04 (2011) 311–314.
[57] Q.P. Yang, L.F. Wang, W.F. Zhang, H. Lu, The fracture analysis of the last stage blade in turbine, Manuf. Inf. Eng. China 13 (2011) 72–73.
[58] Z. Mazur, R. Garcia-Illescas, J. Aguirre-Romano, N. Perez-Rodriguez, Steam turbine blade failure analysis, Eng. Fail. Anal. 15 (1–2) (2008) 129–141.
[59] Z. Mazur, R. García-Illescas, J. Porcayo-Calderón, Last stage blades failure analysis of a 28 MW geothermal turbine, Eng. Fail. Anal. 16 (4) (2009) 1020–1032.
[60] J. Kubiak, G. Urquiza, J.A. Rodriguez, G. González, I. Rosales, G. Castillo, et al., Failure analysis of the 150 MW gas turbine blades, Eng. Fail. Anal. 16 (6) (2009) 1794–1804.
[61] D.Q. Chen, Fracture analysis of rotating blades for a flue gas turbine, Corros. Sci. Prot. Technol. 04 (2005) 275–278.
[62] C.L. Hao, J.X. Dong, M.C. Zhang, C.M. Hong, Failure analysis of gas turbine tenon, Fail. Anal. Prev. 04 (2006) (34-7 + 26).
[63] X.Y. Gai, J. Chen, J.H. Sun, W.L. Zhao, X.M. Guan, A fracture failure analysis of blade in YLII-10,000 K flue gas turbine, Phys. Test. Chem. Anal. A (Phys. Test.) 41 (z1) (2005) 376–381.
[64] L.M. Chen, Y. Wang, M.R. Zhang, L.Z. Yang, The blast furnace gas turbine rotor blade crack analysis, Phys. Test. Chem. Anal. A (Phys. Test.) 41 (z1) (2005) 381–385.
[65] T.L. Han, Z.J. Ruan, C.N. Chen, B.S. Qi, Failure analysis of the turbine blade, Heat Treat. Met. S1 (2007) 159–162.
[66] Y.H. Hu, Y.J. Tian, C.N. Chen, Z.J. Ruan, Z. Zhang, Q.P. Zhong, et al., Failure analysis on laser cladding repaired GH864 alloy rotating blades of flue gas turbines, Heat Treat. Met. 05 (2008) 96–99.
[67] Y.H. Hu, Y.J. Tian, M. Su, Z.J. Ruan, Z. Zhang, Q.P. Zhong, Fracture analysis on the blade of a gas turbine, Heat Treat. Met. S1 (2007) 184–186.
[68] F. Li, Y.T. He, H.P. Li, K.M. Ma, Failure analysis for compressor blade of the fourth stage in an aero-engine, J. Mater. Eng. S1 (2006) 382–384.
[69] W.M. Wu, Y.X. Gu, W.J. Du, Fracture analysis of the rotor blade of stage I on a compressor, Fail. Anal. Prev. 01 (2006) 61–64.
[70] Q.Q. Liu, Fracture analysis on rotor blades of compressor I for a series engines, Fail. Anal. Prev. 02 (2007) (34-6 + 15).
[71] J.X. Zang, M.Y. Bai, T. Jiang, Z.C. Chen, Failure analysis of compressor blades, Fail. Anal. Prev. 02 (2008) 21–25.
[72] F. Lv, G. Fu, Z. Cai, D. Zhang, Failure analysis of components in compressor vane, Eng. Fail. Anal. 16 (5) (2009) 1703–1710.
[73] T. Jiang, C.G. Ji, B. Zhang, Fracture analysis of compressor rotor blade in engine, Equip. Environ. Eng. 03 (2011) 18–22.
[74] N. Ejaz, I. Salam, A. Tauqir, Fatigue failure of a centrifugal compressor, Eng. Fail. Anal. 14 (7) (2007) 1313–1321.
[75] V. Infante, J.M. Silva, M. de Freitas, L. Reis, Failures analysis of compressor blades of aeroengines due to service, Eng. Fail. Anal. 16 (4) (2009) 1118–1125.
[76] L. Witek, M. Wierzbińska, A. Poznańska, Fracture analysis of compressor blade of a helicopter engine, Eng. Fail. Anal. 16 (5) (2009) 1616–1622.
[77] Z.M. Yu, G.R. Fu, A fracture failure analysis of the first stage blade in aeroengine compressor, Phys. Test. Chem. Anal. A (Phys. Test.) 41 (z1) (2005) 369–371.
[78] S. Barella, M. Boniardi, S. Cincera, P. Pellin, X. Degive, S. Gijbels, Failure analysis of a third stage gas turbine blade, Eng. Fail. Anal. 18 (1) (2011) 386–393.
[79] G.H. Farrahi, M. Tirehdast, E. Masoumi Khalil Abad, S. Parsa, M. Motakefpoor, Failure analysis of a gas turbine compressor, Eng. Fail. Anal. 18 (1) (2011) 474–484.
[80] A. Kermanpur, Amin H. Sepehri, S. Ziaei-Rad, N. Nourbakhshnia, M. Mosaddeghfar, Failure analysis of Ti6Al4V gas turbine compressor blades, Eng. Fail. Anal. 15 (8) (2008) 1052–1064.
[81] V.N. Shlyannikov, B.V. Iltchenko, N.V. Stepanov, Fracture analysis of turbine disks and computational–experimental background of the operational decisions, Eng. Fail. Anal. 8 (5) (2001) 461–475.
[82] N.S. Xi, P.D. Zhong, H.Q. Huang, H. Yan, C.H. Tao, Failure investigation of blade and disk in first stage compressor, Eng. Fail. Anal. 7 (6) (2000) 385–392.
[83] K.-S. Song, S.-G. Kim, Y.-H. Hwang, Failure of the J79 engine compressor blade due to stall, J. Fail. Anal. Prev. 7 (3) (2007) 212–217.
[84] P.D. Zhong, X.L. Liu, W.F. Zhang, The failure reason analysis of the third stage turbine blade in an turboprop, Phys. Test. Chem. Anal. A (Phys. Test.) 41 (z1) (2005) 386–389.
[85] X.L. Liu, J.S. Zhou, P.D. Zhong, W.F. Zhang, Fracture failure analysis of the third class turbine vanes in some engine, Mater. Mech. Eng. 08 (2005) 67–70.
[86] S.K. Bhaumik, M. Sujata, M.A. Venkataswamy, M.A. Parameswara, Failure of a low pressure turbine rotor blade of an aeroengine, Eng. Fail. Anal. 13 (8) (2006) 1202–1219.
[87] H. Wang, H.F. Zuo, X. He, Q.H. Lin, X.S. Hu, Failure analysis of 3rd turbine blade of aero-engines, Fail. Anal. Prev. 01 (2007) 24–28.
[88] M. Park, Y.-H. Hwang, Y.-S. Choi, T.-G. Kim, Analysis of a J69-T-25 engine turbine blade fracture, Eng. Fail. Anal. 9 (5) (2002) 593–601.
[89] E. Silveira, G. Atxaga, A.M. Irisarri, Failure analysis of two sets of aircraft blades, Eng. Fail. Anal. 17 (3) (2010) 641–647.
[90] E. Silveira, G. Atxaga, E. Erauzkin, A.M. Irisarri, Study on the root causes for the premature failure of an aircraft turbine blade, Eng. Fail. Anal. 16 (2) (2009) 639–647.
[91] N. Ejaz, A. Tauqir, Failure due to structural degradation in turbine blades, Eng. Fail. Anal. 13 (3) (2006) 452–463.
[92] W.F. Zhang, Y. Li, G. Liu, A.G. Zhao, C.H. Tao, J.F. Tian, et al., Recrystallization and fatigue failure of DS alloy blades, Eng. Fail. Anal. 11 (3) (2004) 429–437.
[93] X.J. Yan, Y. Deng, R.J. Sun, J.W. Xie, Study of fatigue property variation at different regions on a DS turbine blade, Acta Aeronaut. Astronaut. Sin. 10 (2011) 1930–1936.
[94] W.F. Zhang, W. Gao, A.G. Zhao, C.H. Tao, J.F. Tian, G. Yao, Recrystallization and fatigue failure of blades made of a directionally solidified alloy, Acta Aeronaut. Astronaut. Sin. 04 (2003) 377–381.

[95] Y.H. He, X.Q. Hou, C.H. Tao, F.K. Han, Recrystallization and fatigue fracture of single crystal turbine blades, Eng. Fail. Anal. 18 (3) (2011) 944–949.
[96] K.-S. Song, S.-G. Kim, D. Jung, Y.-H. Hwang, Analysis of the fracture of a turbine blade on a turbojet engine, Eng. Fail. Anal. 14 (5) (2007) 877–883.
[97] N.X. Hou, W.X. Gou, Z.X. Wen, Z.F. Yue, The influence of crystal orientations on fatigue life of single crystal cooled turbine blade, Mater. Sci. Eng. A 492 (1–2) (2008) 413–418.
[98] H. Kim, Study of the fracture of the last stage blade in an aircraft gas turbine, Eng. Fail. Anal. 16 (7) (2009) 2318–2324.
[99] N.J. Lourenço, M.L.A. Graça, L.A.L. Franco, O.M.M. Silva, Fatigue failure of a compressor blade, Eng. Fail. Anal. 15 (8) (2008) 1150–1154.
[100] Y.H. He, C.K. Liu, B. Zhang, Fracture analysis of rotor blade of titanium alloy TC11, Chin. J. Nonferrous Met. S1 (2010) 365–368.
[101] I. Le May, Case studies of three fatigue failure evaluations in aircraft, Procedia Eng. 2 (1) (2010) 59–64.
[102] C. Liu, B. Zhang, S. Yang, Y. He, C. Tao, Analysis of fracture and cracks of single crystal blades in aero-engine, Eng. Fail. Anal. 18 (2) (2011) 582–589.
[103] S. Qu, C.M. Fu, C. Dong, J.F. Tian, Z.F. Zhang, Failure analysis of the 1st stage blades in gas turbine engine, Eng. Fail. Anal. 32 (0) (2013) 292–303.
[104] Yuan Z., Zhao, A.G., Tao, C.H., Li, Y.J. Analysis on blade fracture and cause for the incident of a gas turbine. J. Mater. Eng. 2003;(z1): 131–4.
[105] T. Jiang, R.D. Xue, G.Y. Liu, W.F. Zhang, Fracture failure analysis for turbine blades of II stage, J. Mater. Eng. z1 (2003) 162–165.
[106] Y.-S. Choi, K.-H. Lee, Investigation of blade failure in a gas turbine, J. Mech. Sci. Technol. 24 (10) (2010) 1969–1974.
[107] G.M. Song, Fracture analysis on low-pressure compressor rotor blade of gas turbine, Fail. Anal. Prev. 01 (2012) 29–32.
[108] X.H. Cui, B.T. Zhu, S.T. Liu, L.Y. Tang, C.X. Wang, Crack failure analysis of No.1 stage blade for a gas turbine power plant compressor, Fail. Anal. Prev. 03 (2006) 22–26.
[109] A. Troskolanski, The Calculation and Structure of Vane Pumps Beijing, China Machine Press, 1981.
[110] N.S. Vyas, Sidharth, J.S. Rao, Dynamic stress analysis and a fracture mechanics approach to life prediction of turbine blades, Mech. Mach. Theory 32 (4) (1997) 511–527.
[111] X.F. Guan, Z.S. Yao, The Strength Calculation of Pump Parts, China Machine Press, 1981.
[112] X.F. Guan, Modern Pump Technical Manual Beijing, China Astronautic Publishing House, 1995.
[113] S. Aksoy, B. Mitlin, H. Borowy, Structural evaluation and testing of swept compressor rotor, J. Eng. Gas Turbines Power 116 (1) (1994) 217–222.
[114] R. Huang, L.G. Meng, H. Zhang, LCF strength calculating and analyzing of turbocharger compressor wheel, Chin. Intern. Combustion Engine Eng. 04 (2006) 55–57.
[115] J. Liu, Research on Strength Analysis and Structure Improvement Design of the First Stage Impeller in Centrifugal Compressor With Large Flow Rate(Master) Dalian University of Technology, 2009.
[116] Z.H. Song, C.B. Xiong, G.H. Zheng, The Strength Design of Aviation Gas Turbine Engine, Beihang University Press, Beijing, 1988.
[117] J. Kirkhope, G. Wilson, Analysis of Coupled Blade–Disc Vibration in Axial Flow Turbines and Fans, 12th Structures, Structural Dynamics and Materials Conference1971.
[118] J. Hou, B.J. Wicks, R.A. Antoniou, An investigation of fatigue failures of turbine blades in a gas turbine engine by mechanical analysis, Eng. Fail. Anal. 9 (2) (2002) 201–211.
[119] J.A. Kenyon, J.H. Griffin, D.M. Feiner, Maximum bladed disk forced response from distortion of a structural mode, J. Turbomach. 125 (2) (2003) 352–363.
[120] T.S. Luo, R. Dai, Modal analysis of integrated radial inflow impeller with finite element method, Chin. Intern. Combustion Engine Eng. 01 (2005) 77–80.
[121] L.X. Tang, X.D. Lai, J.Q. Zhou, G.H. Shao, The structure static analysis of impeller parts in a centrifugal pump, J. Xihua Univ. (Nat. Sci.) 03 (2008) (11-3 + 7).
[122] Y. Wang, The Rotating Stall Analysis of the First Stage in a Centrifugal CompressorMaster Dlian University of Technology, 2008.
[123] W.Q. Liu, Fatigue Analysis of Weld Impeller of Centrifugal CompressorMaster Dalian University of Technology, 2008.
[124] L.Q. Peng, Research on Fatigue Life of Large Gas Turbine BladeMaster Dalian University of Technology, 2008.
[125] Y.F. Duan, An Analysis of Fatigue Life and Crack Propagation of Aero-Engine Centrifugal ImpellerMaster Hunan University, 2010.
[126] Q. Li, J. Piechna, N. Müeller, Simulation of fatigue failure in composite axial compressor blades, Mater. Des. 32 (4) (2011) 2058–2065.
[127] C. Li, L.K. Ai, S.M. Qu, L.J. Ai, Strength analysis based on coupling stress of high-speed rotary turboexpander impeller with finite element method, Fluid Mach. 02 (2012) 15–19.
[128] B.T. Zhu, The characteristics of dynamic stress and fatigue life of steam turbine's last stage blade under the condition of variable load operation, Shanghai Turbine 01 (2001) 38–42.
[129] Y.H. Xie, Q.J. Meng, Numerical model for steam turbine blade fatigue life, J. Xi'an Jiaotong Univ. 09 (2002) 912–915.
[130] N. Fu, The Strength Analysis and the Fatigue Life Calculation of Blade and Disc in Aero-EngineMaster Northwestern Polytechnical University, 2006.
[131] J.W. Lin, Fatigue Life and Reliability Study on Aviation Engine BladeMaster Tianjin University, 2009.
[132] E. Poursaeidi, A. Babaei, M.R. Mohammadi Arhani, M. Arablu, Effects of natural frequencies on the failure of R1 compressor blades, Eng. Fail. Anal. 25 (0) (2012) 304–315.
[133] W.Y. Zhao, J.Z. Zhang, C.W. Zhou, Study on the vibration localization in the centrifugal impeller with periodic structures, Chin. J. Appl. Mech. 06 (2012) (699-704 + 75).
[134] B.-W. Huang, Effect of number of blades and distribution of cracks on vibration localization in a cracked pre-twisted blade system, Int. J. Mech. Sci. 48 (1) (2006) 1–10.
[135] J.J. Wang, J.D. Xu, Q.H. Li, Analytical models of mistuned bladed disk assembles — a review, Turbine Technol. 04 (2004) 256–259.
[136] J.J. Wang, C.B. Yu, J.Y. Yao, Q.H. Li, Vibratory mode localization factors of mistuned bladed disk assemblies, J. Propul. Technol. 04 (2009) (457-61 + 73).
[137] Z.B. Zhao, E.M. He, H.J. Wang, Correlation between frequency veering and vibration mistuning sensitivity of a bladed disk, Mech. Sci. Technol. 12 (2010) 1606–1611.
[138] S.T. Li, Q.Y. Xu, Fluid induced vibration and dynamic fatigue in centrifugal impeller, Chin. J. Appl. Mech. 03 (2007) (353-8 + 500).
[139] Y.J. Mao, D.T. Qi, Q.Y. Xu, Numerical study on high cycle fatigue failure of a centrifugal compressor impeller blades, J. Xi'an Jiaotong Univ. 11 (2008) 1336–1339.
[140] S.T. Wei, C. Pierre, Localization phenomena in mistuned assemblies with cyclic symmetry part I: free vibrations, J. Vib. Acoust. 110 (4) (1988) 429–438.
[141] S.T. Wei, C. Pierre, Localization phenomena in mistuned assemblies with cyclic symmetry part II: forced vibrations, J. Vib. Acoust. 110 (4) (1988) 439–449.
[142] C. Pierre, D.V. Murthy, Aeroelastic modal characteristics of mistuned blade assemblies: mode localization and loss of eigenstructure, AIAA J. 30 (10) (1992) 2483–2496.
[143] B.C. Watson, M.P. Kamat, Analysis of mistuned cyclic systems using mistune modes, Appl. Math. Comput. 67 (1–3) (1995) 61–79.
[144] T. Krzyżyński, K. Popp, W. Sextro, On some regularities in dynamic response of cyclic periodic structures, Chaos, Solitons Fractals 11 (10) (2000) 1597–1609.
[145] H.H. Yoo, J.Y. Kim, D.J. Inman, Vibration localization of simplified mistuned cyclic structures undertaking external harmonic force, J. Sound Vib. 261 (5) (2003) 859–870.
[146] C. Hu, F.M. Li, J.X. Zou, W.H. Huang, A study on localization of vibration mode in mistuned bladed disk assemblies, Proc. CSEE 11 (2003) 193–198.
[147] C.Y. Zhou, J.X. Zou, Direct prediction of the effects of mistuning on vibration of bladed disc assemblies, Acta Aeronaut. Astronaut. Sin. 05 (2001) 465–467.
[148] Z.J. Ding, Research on Dynamic Characteristics of Blade With Cracks and Monitoring System for Fatigue TestMaster Nanjing University of Aeronautics and Astronautics, 2009.
[149] L. Witek, Crack growth simulation in the compressor blade subjected to vibration using boundary element method, 14th Polish Conference on Fracture Mechanics and Fatigue, September 23, 2013–September 26, 2013, Trans Tech Publications Ltd, Kielce-Cedzyna, Poland 2014, pp. 261–268.
[150] A. Hutson, T. Nicholas, R. John, Fretting fatigue crack analysis in Ti–6Al–4V, Int. J. Fatigue 27 (10–12) (2005) 1582–1589.
[151] D.Y. Hu, R.Q. Wang, J. Deng, Crack growth life prediction based on finite element method, J. Mech. Strength 31 (2) (2009) 264–268.
[152] M.R. Nami, H. Eskandari, Stress intensity factors in a rotating impeller containing semi-elliptical surface crack, Mech. Based Des. Struct. Mach. 40 (1) (2012) 1–18.
[153] Y.F. Gao, W.B. Hu, Z.X. Wen, Z.F. Yue, L. Chen, Stress field and propagation trend of crack tip in tenon of nickel-based single crystal superalloys turbine blade, J. Aerosp. Power 29 (3) (2014) 612–618.
[154] H.Y. Liu, The Analysis of Service Environment and Fatigue Crack Growth in Determination of Critical Threshold of Impeller RemanufacturingMaster Dalian University of Technology, 2014.

[155] L. Witek, Simulation of crack growth in the compressor blade subjected to resonant vibration using hybrid method, Eng. Fail. Anal. 49 (2015) 57–66.
[156] K.W. Barlow, R. Chandra, Fatigue crack propagation simulation in an aircraft engine fan blade attachment, Fatigue Damage of Structural Materials V, September 19, 2004–September 24, 2004, Elsevier Ltd 2005, pp. 1661–1668.
[157] E. Poursaeidi, M. Salavatian, Fatigue crack growth simulation in a generator fan blade, Eng. Fail. Anal. 16 (3) (2009) 888–898.
[158] E. Poursaeidi, H. Bakhtiari, Fatigue crack growth simulation in a first stage of compressor blade, Eng. Fail. Anal. 45 (2014) 314–325.
[159] L. Witek, Numerical stress and crack initiation analysis of the compressor blades after foreign object damage subjected to high-cycle fatigue, Eng. Fail. Anal. 18 (8) (2011) 2111–2125.
[160] M. Holl, T. Rogge, S. Loehnert, P. Wriggers, R. Rolfes, 3D multiscale crack propagation using the XFEM applied to a gas turbine blade, Comput. Mech. 53 (1) (2014) 173–188.
[161] C.G. Li, E.J. Liu, B. Hao, L. Hao, Development of thermal mechanical fatigue test rig, Aeroengine 03 (2004) (8-10 + 4).
[162] M.X. Yan, Y.K. Tang, G.C. Chen, The design and development of impeller fatigue testing machine based on VB, Mech. Manuf. 02 (2010) 32–35.
[163] X.J. Yan, J.X. Nie, The Fatigue of Turbine Blade, Science Press, Beijing, 2014.
[164] G.C. Hou, Z.H. Yu, Q. Li, An investigation on low cycle fatigue life of engine 1st stage turbine blades, Gas Turbine Exp. Res. 04 (2002) 25–28.
[165] W. Li, H.Q. Shi, Research on experimental technique for fatigue-creep life of the turbine blade in aeroengine, J. Aerosp. Power 04 (2001) 323–326.
[166] H.B. Wang, Test methods on thermal/mechanical fatigue (TMF) of turbine blade, Aeroengine 02 (2007) 7–11.
[167] S. Weser, U. Gampe, M. Raddatz, R. Parchem, P. Lukas, Advanced experimental and analytical investigations on combined cycle fatigue (CCF) of conventional cast and single-crystal gas turbine blades, ASME 2011 Turbo Expo: Turbine Technical Conference and Exposition, GT2011, June 6, 2011–June 10, 2011, American Society of Mechanical Engineers, Vancouver, BC, Canada 2011, pp. 19–28.
[168] Z.H. Gao, R.Q. Sun, Y.Y. Xu, W.Z. Jiang, Fatigue tests of blade specimens with different anti water erosion processes, Therm. Turbine 02 (1984) 23–29.
[169] Q.X. Lu, T.Y. Wu, An automated fatigue test system, Acta Aeronaut. Astronaut. Sin. 05 (1985) 474–477.
[170] Z.H. Xu, An experimental investigation of a new type of equipment for fatigue test, J. Nanjing Aeronaut. Inst. 01 (1987) 123–130.
[171] J.Y. Hou, S. Zheng, X.Y. Huang, The vibration fatigue behaviour of blades and samples of titanium alloy TC11, J. Mater. Eng. 06 (1988) 2–6.
[172] Z.D. Sun, Q.X. Lu, Effect of foreign object damage on the life of compressor blades, Acta Aeronaut. Astronaut. Sin. 06 (1990) 253–260.
[173] J.D. Kang, S.X. Chen, Z.H. Xu, Residual vibration fatigue life of compressor blade damaged by foreign object, J. Aerosp. Power 03 (1998) (107-9 + 28-29).
[174] J.M. Cai, Z.X. Li, C.X. Cao, X. Huang, Q. Lei, Y.W. Zhang, Effect of Nd-rich particles on room temperature vibration fatigue of Ti60 titanium alloy, J. Mater. Eng. 08 (2007) 57–60.
[175] A.H. Hu, K.M. Ma, Investigation on vibration characteristics of 4th compressor blades in an aero-engine, Fail. Anal. Prev. 04 (2006) 10–12.
[176] H.B. Miao, X.L. Liu, Failure analysis of high-pressure compressor blades in aero-engine, Heat Treat. Met. S1 (2007) 79–83.
[177] L. Wan, S.M. Li, Y.Z. Jin, Fatigue test of an aeroengine compressor IGVs, Aeroengine 03 (2008) 15–17.
[178] Z.P. Zhang, Q. Sun, C.W. Li, Y.J. Qiao, W.Z. Zhao, Relationship between fatigue life and af value for aero-engine compressor blades, Chin. J. Appl. Mech. 03 (2006) (459-61 + 514).
[179] B.B. Zhao, L. Cheng, C. Gao, Study of resonant frequency and fatigue life of blade based on BP neural network, Turbine Technol. 06 (2010) 440–442.
[180] D.M. Zhang, E.J. Liu, A new approach of the vibration endurance test at high temperature for engine turbine blade, Aeroengine 01 (2005) 18–21.
[181] H.B. Nie, Steam Turbine Blade Vibration Fatigue Test and Automatic Control System DevelopmentMaster Zhejiang University, 2006.
[182] C. Shao, S. Ge, An assumption of material fatigue test in high frequency vibration environment, Struct. Strength Res. 2 (2009) 11–15.
[183] L. Witek, Experimental crack propagation and failure analysis of the first stage compressor blade subjected to vibration, Eng. Fail. Anal. 16 (7) (2009) 2163–2170.
[184] L. Witek, Crack propagation analysis of mechanically damaged compressor blades subjected to high cycle fatigue, Eng. Fail. Anal. 18 (4) (2011) 1223–1232.
[185] J. Li, Q. Sun, C.W. Li, J. Liu, Z.P. Zhang, Study on the vibration fatigue life for aero-engine compressor blade, Chin. J. Appl. Mech. 02 (2011) (189-93 + 217).
[186] Q.T. Li, Q.C. Liu, J.S. Shen, L. Cheng, C. Gao, W. Chen, Experiment on ultra-high cycle bending vibration fatigue of titanium alloy TC17, J. Aerosp. Power 03 (2012) 617–622.
[187] P. Wang, M. Hou, Integral Impeller Blade Vibration Fatigue Test Device and Test Method(CN103196644A. China) 2013.
[188] F.J. Xu, J.X. Nie, C.Z. Zhao, A compound fatigue investigation of plate specimen under low-cycle load superposed on high cycle load, J. Aerosp. Power 02 (1992) (121-4 + 92).
[189] X.F. Li, Analysis of the high temperature high-and-low-cycle fatigue life of 3rd stage turbine blades of some engine, Machine Building & Automation 03 (2010) (11-2 + 36).
[190] D.Q. Shi, Y.Y. Luo, X.G. Yang, A Kind of Biaxial High–Low Cycle Complex Fatigue Test Device(CN103076246A. China) 2013.
[191] R.J. Sun, X.J. Yan, J.X. Nie, Failure characteristics of directional solidification turbine blade under high temperature low cycle fatigue load, Acta Aeronaut. Astronaut. Sin. 02 (2011) 337–343.
[192] R.Q. Wang, F.L. Jing, G.C. Hou, D.Y. Hu, J. Fan, X.L. Shen, A Thermal Mechanical Fatigue Test System for Hollow Air-Cooled Turbine Blade(CN102539135A. China) 2011.
[193] R.Q. Wang, D.Y. Hu, G.C. Hou, X.L. Shen, Turbine Disk/Blade Mortise High Temperature Composite Fatigue Loading Method and Device(CN101464240. China) 2009.
[194] R.Q. Wang, J.X. Nie, Combined fatigue experimental study of firtree mortises on light/serious corrosive turbine disc at elevated temperature, J. Propul. Technol. 04 (1998) 111–115.
[195] X.J. Yan, J.X. Nie, New experimental approach in determining creep/fatigue life of directionally solidified alloy turbine blade, J. Aerosp. Power 06 (2005) 925–931.
[196] X.J. Yan, R.J. Sun, Y. Deng, Z.N. Liu, J.X. Nie, Experimental study on fatigue curve law of turbine blade under combined high and low cycle loading, J. Aerosp. Power 08 (2011) 1824–1829.
[197] C.J. Cross, Multiaxial testing of gas turbine engine blades, 36th AIAA/ASME/SAE/ASEE Joint Propulsion Conference and Exhibit 2000, July 16, 2000–July 19, 2000, American Institute of Aeronautics and Astronautics Inc., Huntsville, AL, United states, 2000.
[198] T. Ogata, M. Yamamoto, Life evaluation of IN738LC under biaxial thermo-mechanical fatigue, Proceedings of the Sixth International Conference on Biaxial and Multiaxial Fatigue and Fracture 2001, pp. 839–848.
[199] M. Xie, S.R. Soni, C.J. Cross, Terborg G.E., Multiaxial High Cycle Fatigue Test System(US6718833. USA) 2004.
[200] W.Q. Wang, P.F. Wang, M. Zhang, Y. Liu, J.F. Li, A Static Fatigue Test Method Based on Vibration Table Combined With Accessories(201410271461.2.China) 2014.